OPEN ACCESS

TRANSLATIONAL SCIENCE

Deletion of activin A in mesenchymal but not myeloid cells ameliorates disease severity in experimental arthritis

Vanessa Waltereit-Kracke, Corinna Wehmeyer, Denise Beckmann, Eugenie Werbenko, Julia Reinhardt, Fabienne Geers, Mike Dienstbier, Michelle Fennen, Johanna Intemann, Peter Paruzel, Adelheid Korb-Pap, Thomas Pap, Berno Dankbar

Handling editor Josef S Smolen

► Additional supplemental material is published online only. To view, please visit the journal online (http://dx.doi.org/10.1136/annrheumdis-2021-221409).

Institute of Musculoskeletal Medicine, University Hospital Muenster, Muenster, Nordrhein-Westfalen, Germany

Correspondence to
Dr Berno Dankbar, University Hospital Munster, Munster, Nordrhein-Westfalen, Germany; dankbarb@uni-muenster.de

Received 25 August 2021
Accepted 6 April 2022
Published Online First 13 April 2022

ABSTRACT

Objective The aim of this study was to assess the extent and the mechanism by which activin A contributes to progressive joint destruction in experimental arthritis and which activin A-expressing cell type is important for disease progression.

Methods Levels of activin A in synovial tissues were evaluated by immunohistochemistry, cell-specific expression and secretion by PCR and ELISA, respectively. Osteoclast (OC) formation was assessed by tartrat-resistant acid phosphatase (TRAP) staining and activity by resorption assay. Quantitative assessment of joint inflammation and bone destruction was performed by histological and micro-CT analysis. Immunoblotting was applied for evaluation of signalling pathways.

Results In this study, we demonstrate that fibroblast-like synoviocytes (FLS) are the main producers of activin A in arthritic joints. Most significantly, we show for the first time that deficiency of activin A in arthritic FLS (ActβA$^{d/d}$ ColVI-Cre) but not in myeloid cells (ActβA$^{d/d}$ LysM-Cre) reduces OC development in vitro, indicating that activin A promotes osteoclastogenesis in a paracrine manner. Mechanistically, activin A enhanced OC formation and activity by promoting the interaction of activated Smad2 with NFATc1, the key transcription factor of osteoclastogenesis. Consistently, ActβA$^{d/d}$ LysM-Cre hTNFtg mice did not show reduced disease severity, whereas deficiency of activin A in ColVI-Cre-expressing cells such as FLS highly diminished joint destruction reflected by less inflammation and less bone destruction.

Conclusions The results highly suggest that FLS-derived activin A plays a crucial paracrine role in inflammatory joint destruction and may be a promising target for treating inflammatory disorders associated with OC formation and bone destruction like rheumatoid arthritis.

Key messages

What is already known about this subject?
⇒ High levels of activin A in serum, synovial fluid and synovial tissue of patients with rheumatoid arthritis (RA) were observed.
⇒ Activin A promotes osteoclast development.

What does this study add?
⇒ Fibroblast-like synoviocytes (FLS) seem to be the main producer of activin A in arthritic joints.
⇒ Deletion of activin A in FLS but not in myeloid cells highly diminishes joint pathology in experimental arthritis displayed by less inflammation and less bone destruction, confirming for the first time a significant role for activin A in arthritis development in vivo.

How might this impact on clinical practice or future developments?
⇒ Blockade of activin A or corresponding signalling pathways may be a promising treatment option for diseases associated with inflammatory bone destruction such as RA.

INTRODUCTION

Rheumatoid arthritis (RA) is a common type of inflammatory arthritis characterised by chronic inflammation, culminating in destruction of the joint. In the pathological state of RA, the synovial lining layer becomes hyperplastic due to influx of macrophage-like synoviocytes and increased cell division of fibroblast-like synoviocytes (FLS).[1–3] The continuous presence of cytokines, chemokines, growth factors and other molecular mediators leads to the activation of FLS resulting in an aggressive tumor-like transformation[4 5] contributing to pannus formation, a highly destructive tissue located at the interface between synovium, cartilage and bone. FLS and macrophages predominate this tissue and mediate the process of joint destruction by expression of degradative enzymes including matrix metalloproteinases and collagenases.[6]

However, bone destruction is mediated by osteoclasts (OCs) located at the interface between the pannus and periarticular bone surface.[7] Many factors such as tumour necrosis factor alpha (TNF-α), interleukin (IL)-1, IL-6, IL-17 and receptor activator of nuclear factor κB ligand (RANKL) produced directly by FLS or within the pannus tissue by infiltrated immune cells are able to enhance the differentiation of cells of the monocyte–macrophage lineage into OC, thereby disturbing the balance of bone remodelling and shifting the remodelling process towards bone resorption.[7–13]

Another factor shown to influence bone destruction in RA by directly promoting OC formation is activin A.[14–19] Activin A belongs to the transforming growth factor beta (TGF-β)-like group of

Check for updates

To cite: Waltereit-Kracke V, Wehmeyer C, Beckmann D, *et al*. *Ann Rheum Dis* 2022;**81**:1106–1118.

the TGF-β superfamily consisting of two disulfide-linked inhibin βA subunits.[20–22] Interestingly, proinflammatory cytokines such as TNF-α, IL-1β and TGF-β have been found to increase levels of activin A in RA.[23 24] In accordance with this, high levels of activin A in serum, synovial fluid and synovial tissue of patients with RA, compared with patients with osteoarthritis (OA), were observed.[25–28] Besides FLS, activin A is produced also by macrophages[29] and not only is induced by proinflammatory cytokines but in turn also stimulates the production of inflammatory mediators like TNF-α, IL-1β, IL-6, nitric oxide and prostaglandin E_2,[25 28 30 31] suggesting an important role of activin A in the pathology of RA. However, the extent to which activin A influences arthritis development and progression in vivo has not been elucidated so far, and even the most significant activin A-producing cell type involved in disease progression has not yet been identified. Therefore, the aim of this study was to investigate whether activin A contributes to joint inflammation and progressive bone loss in experimental arthritis and which activin A-expressing cell type within the inflamed joint is important for disease progression.

METHODS

Detailed experimental procedures are described in the online supplemental material.

RESULTS

Increased levels of activin A in arthritis

Immunofluorescence staining revealed a higher expression of activin A in the synovial tissues of patients with RA compared with those of patients with OA (2.7-fold). Whereas in OA specimens activin A expression appeared mainly in cells of the synovial lining layer, activin A expression in RA was observed throughout the whole synovial tissue (figure 1A). More detailed analysis demonstrated an increase of activin A-expressing macrophages (2.7-fold), FLS (5.6-fold) and neutrophils (2.6-fold), whereby the latter one was not significant (figure 1C). Consistently, a TNFα-dependent chronic arthritis mouse model (hTNFtg) revealed dramatically increased levels of activin A in the hind paws (3.7-fold, figure 1B) and in sera (7.3-fold, figure 1D) compared with wild-type (WT) mice. Moreover, mRNA of the inhibin βA subunit was abundantly expressed in RA FLS as well as in FLS of arthritic mice (figure 1E). Together, these data indicate that under inflammatory conditions, activin A appears to be highly upregulated and that FLS may be the main producers of activin A within the inflamed synovial tissue.

Since an inflammatory environment obviously causes an increase in activin A levels, WT and hTNFtg mouse FLS were stimulated with the proinflammatory cytokines IL-1α, IL-1β, TGF-β, and IL-17A. Indeed, all cytokines were able to significantly enhance the secretion of activin A compared with untreated controls (4.3-fold to 9.7-fold higher) with the exception of IL-17A, where the secretion of WT FLS was identical to the untreated control (figure 1F). Moreover, hTNFtg FLS showed an even stronger increase in activin A secretion on stimulation with proinflammatory cytokines compared with WT FLS (11.6-fold to 17.5-fold higher, figure 1G). Because of the increased number of activin A-producing macrophages in RA and hTNFtg synovial tissue, regulation of activin A by inflammatory cytokines was additionally analysed in bone marrow-derived macrophages (BMDM). In contrast to FLS, a distinct increase in activin A secretion by BMDMs was exclusively observed on stimulation with TGF-β1, and no significant differences in secretion were found between WT (increase by 4.1) and hTNFtg (increase by 6.5) (figure 1I–K). It should be stressed that BMDMs secreted considerably lower amounts of activin A than FLS (pg/mL vs ng/mL range; figure 1H,K), further supporting the hypothesis that FLS are the main producers of activin A within the inflamed synovium.

Activin a highly enhances OC formation and activity

To investigate the impact of activin A on osteoclastogenesis, primary BMDMs isolated from WT mice were differentiated into OC by stimulation with RANKL, activin A or both (figure 2A). Interestingly, concomitant treatment of BMDMs with RANKL and activin A led to enhanced OC differentiation (2.6-fold, figure 2B) associated with a higher number of nuclei per OC (3.6-fold, figure 2C) as well as an increased OC size (2.5-fold, figure 2D), leading to an increased total OC area (6.9-fold, figure 2E) compared with RANKL treatment alone. Of note, activin A alone was not able to induce OC differentiation (figure 2A). Consistently, resorption analysis revealed an increased formation of resorption pits (figure 2F,G) and total resorption area (figure 2H) on calcium phosphate plates on differentiation with both RANKL and activin A simultaneously compared with the RANKL-treated control (2.6-fold and 5.9-fold, respectively). Most interestingly, the additional increase in resorption area per pit by 2.3-fold compared with the RANKL-treated control clearly demonstrate that the observed higher resorption is not only due to higher OC numbers but also additionally based on increased OC activity (figure 2I). Finally, figure 2J exclude that the higher number of OC on stimulation with activin A was dependent on a higher number of BMDMs or available OC precursors provoked by proliferation.

Altogether, these data indicate that activin A strongly enhances the RANKL-mediated osteoclastic resorption due to increased numbers as well as increased activity of in vitro differentiated primary OCs. In order to bridge to humans, the effects of activin A on human OC differentiation were investigated. Consistent with the effects of activin on murine osteoclastogenesis, activin A also enhanced the RANKL-induced differentiation of human peripheral blood mononuclear cells (PBMCs) into OCs by about 5-fold, associated again with an increase in OC size by about 6-fold, indicating that activin A must be considered an important cross-species factor in OC differentiation (figure 2K).

Since both FLS as well as macrophages produce activin A, we next wanted to unravel whether autocrine or paracrine activin A is important for joint destruction in arthritis. To this end, we compared the impact of activin-deficiency in myeloid cells and FLS on the formation of OCs in vitro as well as on arthritis development and progression in vivo.

Lack of activin A in myeloid cells has no influence on OC differentiation

To confirm a myeloid lineage-specific as well as effective deletion of activin A in the $Actβa^{d/d}$ LysM-Cre mice, activin A secretion by FLS (figure 3A) and myeloid cells (figure 3B) was measured by ELISA. As expected, $Actβa^{d/d}$ LysM-Cre FLS showed no changes in activin A secretion compared with FLS from $Actβa^{flox/flox}$ ($Actβa^{f/f}$) mice, whereas a significant, almost complete reduction of activin A secretion by BM cells, BMDMs, pre-OCs (pOCs) and OC of $Actβa^{d/d}$ LysM-Cre mice was observed, indicating that activin A is effectively deleted in cells of the myeloid lineage but not in mesenchymal cells such as FLS.

To analyse whether activin A deficiency in myeloid cells affects osteoclastogenesis in vitro, BMDMs from $Actβa^{f/f}$ and $Actβa^{d/d}$ LysM-Cre mice as well as from $Actβa^{f/f}$ hTNFtg and $Actβa^{d/d}$

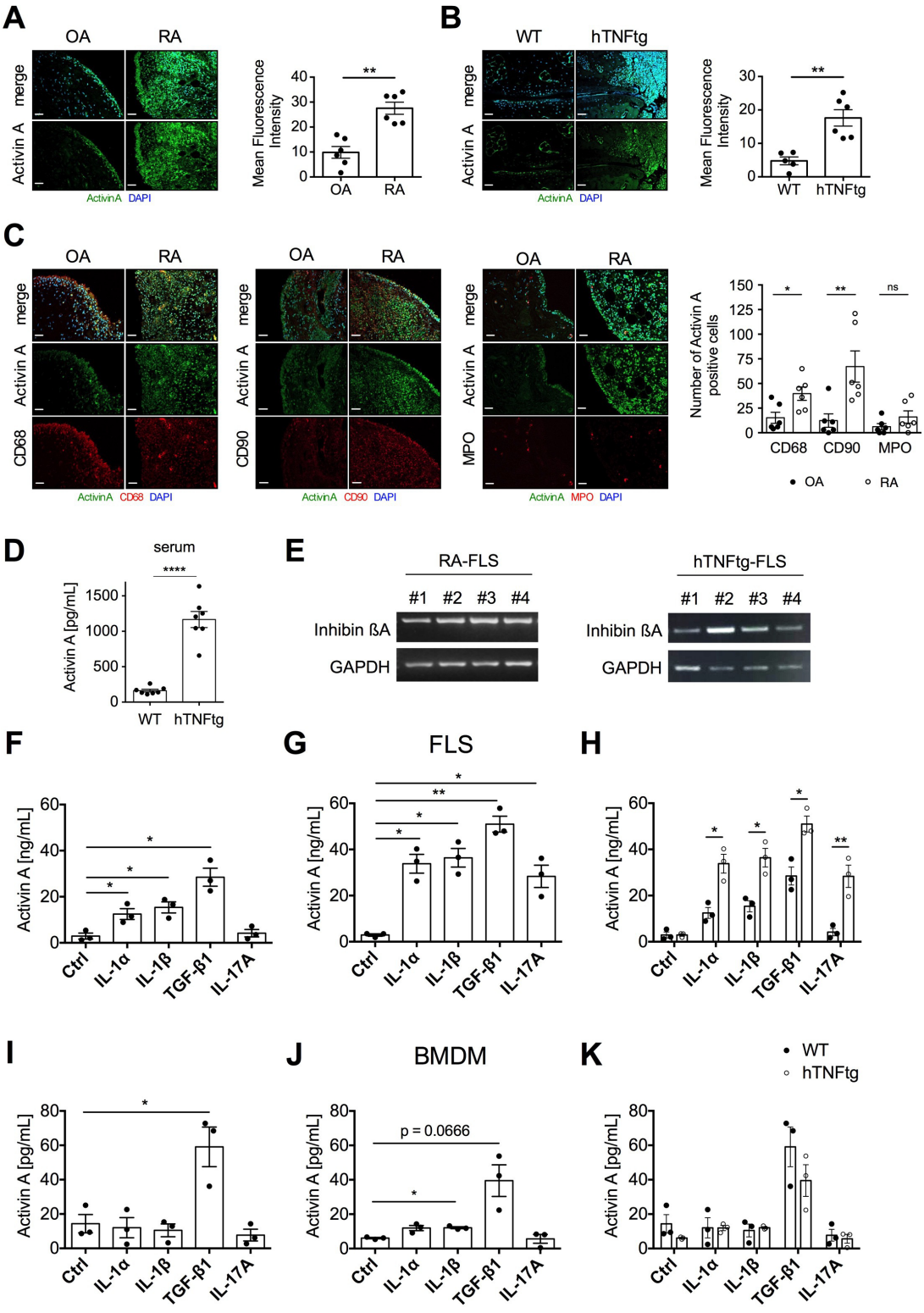

Figure 1 High levels of activin A under inflammatory conditions. (A) representative images of fluorescence stainings of activin A in synovial tissue samples obtained from patients with OA and RA and corresponding quantification (n=6, unpaired t-test**). (B) Representative images of fluorescence stainings of activin A in hind paws of WT and arthritic hTNFtg mice and corresponding quantification (n=5–6, unpaired t-test**). (C) Representative fluorescence costainings of activin A with CD68, CD90 or MPO in synovial tissue samples obtained from patients with OA and RA and quantification of corresponding activin A-positive cells (n=6, unpaired t-test*,**). (D) Activin A concentrations in serum of WT and arthritic hTNFtg mice. Data represent means±SEM (n=7, unpaired t-test****). (E) PCR analysis of inhibin βA-subunit mRNA in FLS of patients with RA (n=4) and of hTNFtg mice (n=4). (F) Secretion of activin A by WT and (G) hTNFtg FLS on stimulation with IL-1α (20 ng/mL), IL-1β (20 ng/mL), TGF-β1 (20 ng/mL) and IL-17A (20 ng/mL) for 48 hours. (H) Comparison of activin A secretion by WT and hTNFtg FLS. (I) Secretion of activin A by WT and (J) hTNFtg BMDMs on stimulation with IL-1α (20 ng/mL), IL-1β (20 ng/mL), TGF-β1 (20 ng/mL) and IL-17A (20 ng/mL) for 48 hours. (K) Comparison of activin A secretion by WT and hTNFtg BMDMs. All data are means±SEM (n=3, paired t-test, comparison WT/hTNFtg unpaired t-test*). *P≤0.05, **P≤0.01, ****P≤0.0001. Ctrl, control; FLS, fibroblast-like synoviocytes; IL, interleukin; ns, not significant; OA, osteoarthritis; RA, rheumatoid arthritis; WT, wild type.

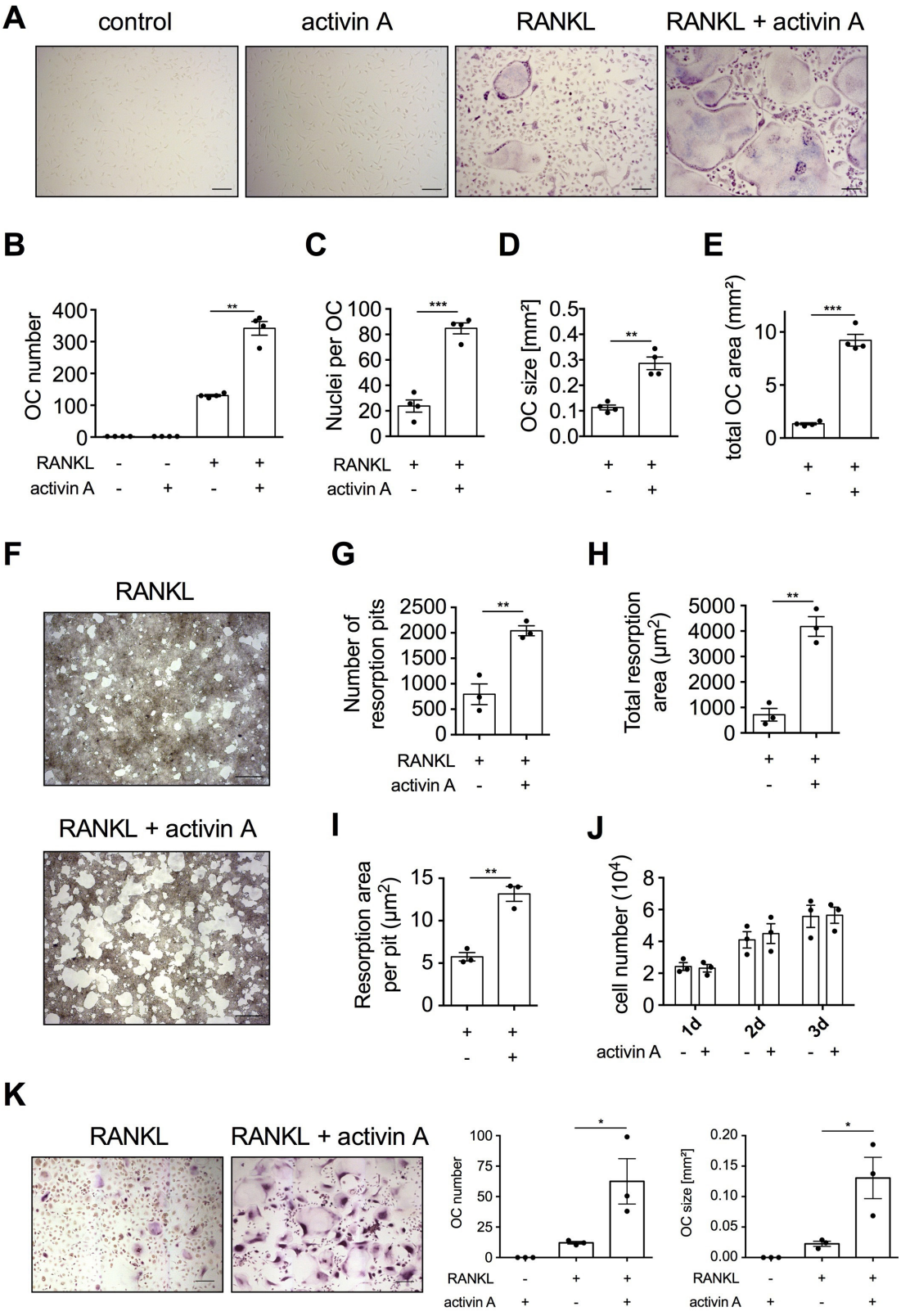

Figure 2 Enhanced RANKL-mediated differentiation and activity of OCs by activin A. (**A**) Representative images of TRAP staining after 4 days of OC differentiation in the presence of 30 ng/mL macrophage colony-stimulating factor (M-CSF, control) together with activin A (30 ng/mL) or RANKL (50 ng/mL) or RANKL plus activin A (scale bar 100 µm). (B) Corresponding OC numbers, (C) number of nuclei per OC, (D) OC size and (E) total OC area per well (n=4). (F) Representative images of resorption pit formation of WT BMDMs after 6 days of OC differentiation using calcium phosphate as substrate on stimulation with RANKL or RANKL plus activin A (scale bar 500 µm). (G) Number of resorption pits, (H) total resorption area and (I) resorption area per pit after 6 days of OC differentiation (n=3). (J) Cell numbers of BMDMs with or without activin A stimulation after 1, 2 and 3 days (n=3). (K) Representative TRAP staining of human OCs after 15 days of differentiation in the presence of M-CSF (30 ng/mL) and RANKL (50 ng/mL) with and without 100 ng/mL activin A (scale bar 200 µm) and corresponding OC number and OC size. All data are means±SEM (t-test). *P≤ 0.05, **P≤0.01, ***P≤ 0.001. OC, osteoclast; RANKL, receptor activator of nuclear factor κB ligand.

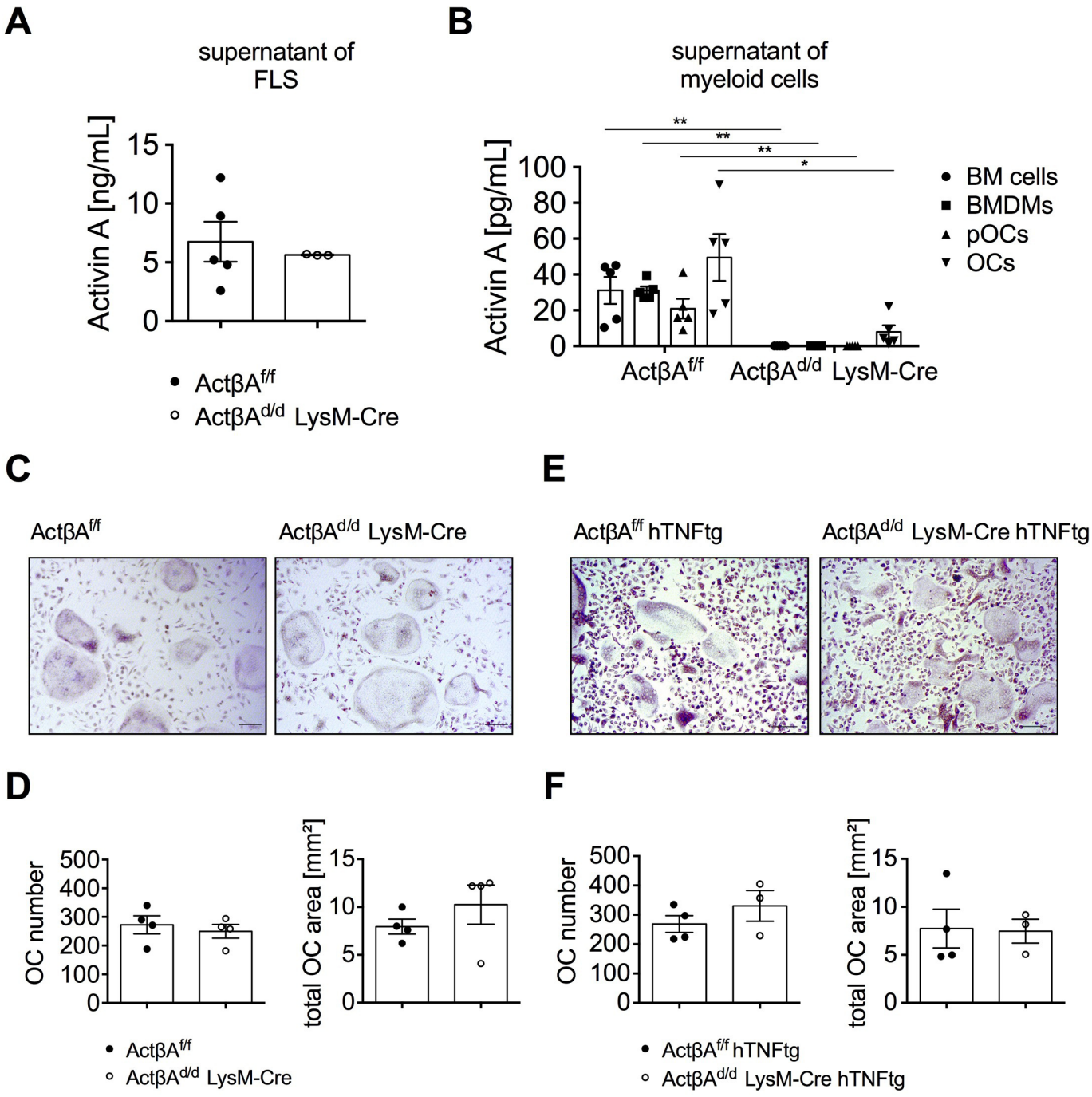

Figure 3 Deficiency of activin A in BMDMs had no impact on OC differentiation in vitro. (A) Secretion of activin A by FLS from ActβA$^{f/f}$ and ActβA$^{d/d}$ LysM-Cre mice after 48 hours. (B) Secretion of activin A by BM cells, BMDMs, pOCs and OCs from ActβA$^{f/f}$ and ActβA$^{d/d}$ LysM-Cre mice after 48 hours. BM cells were not stimulated; BMDMs were stimulated with M-CSF (30 ng/mL) for 3 days; pOCs were stimulated for 3 days with M-CSF (30 ng/mL) followed by stimulation with M-CSF and RANKL (50 ng/mL) for further 2 days. OCs were generated by stimulation of pOCs for a further 2 days with RANKL. All data are means±SEM (n=3–5, Mann-Whitney U test*,**). (C) Representative images of TRAP staining after 5 days of differentiation of BMDMs from ActβA$^{f/f}$ and ActβA$^{d/d}$ LysM-Cre mice (scale bar 100 µm). (D) Corresponding OC number and total OC area per well. All data are means±SEM (n=4, Mann-Whitney U test). (E) Representative images of TRAP staining after 5 days of differentiation of BMDMs from ActβA$^{f/f}$ hTNFtg and ActβA$^{d/d}$ LysM-Cre hTNFtg mice (scale bar 100 µm). (F) Corresponding OC number and total OC area per well. All data are means±SEM (n=4 and 3, respectively; Mann-Whitney U test). *P≤0.05, **P≤0.01. ActβA$^{f/f}$, ActβA$^{flox/flox}$; FLS, fibroblast-like synoviocytes; IL, interleukin; OC, osteoclast; RANKL, receptor activator of nuclear factor κB ligand.

LysM-Cre hTNFtg mice were stimulated with RANKL and subsequently stained for TRAP after 5 days of differentiation (figure 3C,E). Of note, the deficiency of activin A in myeloid cells did not show significant differences in OC number and area neither from non-arthritic (figure 3D) nor from arthritic mice (figure 3F) which leads to the assumption that autocrine activin A is not important for OC differentiation. Because activin levels were rather low, cells were additionally stimulated with TGF-ß1, previously shown to enhance activin secretion in BMDMs (figure 1I,J). However, additional stimulation with TGF-ß1

had no effect on OC formation (online supplemental figure 1). Moreover, to exclude whether residual activin A, due to incomplete deletion in LysM-Cre BMDMs, may interfere with the effects of deletion, cells were additionally treated with activin A antibodies. Indeed, blocking activin A did not influence OC development of ActβA$^{d/d}$ LysM-Cre BMDMs, whereas blocking of myostatin, another member of the TGF-ß superfamily and known to stimulate OC formation, led to decreased OC differentiation (online supplemental figure 4).

Deficiency of activin A in LysM-Cre-expressing cells does not significantly affect disease severity in hTNFtg mice

Taking the involvement of activin A in bone remodelling and inflammation into account, we first asked whether the loss of activin A in cells of the myeloid lineage would influence the development of inflammatory bone destruction in arthritis. Because the complete knockout of activin A is lethal,[32] ActβA$^{f/f}$ mice were used to generate conditional knockouts by breeding these mice with the LysM-Cre mouse line.[33 34] The resulting mice with a cell-specific deletion of activin A (ActβA$^{d/d}$ LysM-Cre) were subsequently cross-bred with hTNFtg mice to generate deleted arthritic mice. hTNFtg mice are overexpressing the hTNFα transgene and thereby develop a chronic destructive arthritis that shares many characteristics with human RA.[35]

As expected, ActβA$^{f/f}$ hTNFtg and ActβA$^{d/d}$ LysM-Cre hTNFtg mice showed an increase in paw swelling (figure 4A) and loss of grip strength (figure 4B) during disease development. However, no significant differences in the clinical symptoms between the two hTNFtg genotypes could be observed during the course of the disease. ActβA$^{f/f}$ and ActβA$^{d/d}$ LysM-Cre showed no signs of arthritis.

Moreover, micro-CT (µCT) and histomorphometry showed no obvious differences in joint destruction as well as OC numbers in 12-week-old arthritic mice with deletion of activin A compared with the hTNFtg mice (figure 4C–E). Quantitative morphometric evaluation confirmed the lack of significant differences in inflammation, bone erosion and OC numbers (figure 4F–H and online supplemental figure 6). However, a tendency towards less inflammation (31.4 %) in the hind paws of activin A-deleted compared with non-deleted hTNFtg mice could be observed. Moreover, evaluation of trabecular and cortical bone parameters in non-arthritic ActβA$^{f/f}$, LysM-Cre and ActβA$^{d/d}$ LysM-Cre mice revealed that activin A also does not influence physiological bone remodelling (online supplemental figure 2). Of note, activin A serum levels were not significantly reduced, although a tendency towards lower levels (about 27%) could be observed in ActßA$^{d/d}$ LysM-Cre hTNFtg mice (online supplemental figure 3A).

Lack of activin A in FLS effectively decreases OC differentiation

In order to analyse the deletion efficiency and specificity of activin A in FLS, secretion of activin A by FLS and myeloid cells was measured via ELISA. As anticipated, ActβA$^{d/d}$ ColVI-Cre FLS showed a significant reduction in activin A secretion by about 85% compared with FLS from ActβA$^{f/f}$ mice (figure 5A). In contrast, activin A secretion by myeloid lineage cells from ActβA$^{d/d}$ ColVI-Cre mice were not significantly reduced compared with those from ActβA$^{f/f}$ mice (figure 5B).

As expected, no differences in OC formation between BMDMs from ActβA$^{f/f}$ and ActβA$^{d/d}$ ColVI-Cre mice,[36] neither of non-arthritc nor of arthritic mice, was observed (figure 5C–F). In contrast, cocultures of BMDMs with FLS from ActβA$^{d/d}$ ColVI-Cre hTNFtg FLS led to the formation of smaller and less OCs compared with the cocultures with ActβA$^{f/f}$ hTNFtg FLS, which generated a higher number of OCs that were also larger in size (figure 5G). Quantitative analysis revealed that the number of OCs and the total OC area were significantly decreased in cocultures with ActβA$^{d/d}$ ColVI-Cre hTNFtg FLS by 25.6% and 36.7 %, respectively, compared with the ActβA$^{f/f}$ hTNFtg FLS, suggesting that activin A is an important paracrine factor for OC formation (figure 5H).

Of importance, FLS do not only express activin A but also myostatin, another member of the TGF-ß superfamily and also a promoting factor for OC differentiation.[37] To clarify the relative contribution of activin and myostatin on OC development, cocultures of arthritic FLS with BMDM in the presence of blocking antibodies against activin A or myostatin were performed. Cocultures with FLS from ActβA$^{f/f}$ hTNFtg mice treated with antibodies against activin A showed a reduction of OC development by about 48%, whereas treatment with antibodies against myostatin showed a tendency towards reduced OC formation (about 20%), pointing to a more important role of paracrine activin A. As expected, the already decreased osteoclastogenesis observed in cocultures with ActβA$^{d/d}$ ColVI-Cre hTNFtg FLS could not be further reduced by anti-activin AB but interestingly, also no further reduction could be seen on treatment with anti-myostatin AB, confirming that activin A is the determining factor in FLS-mediated OC differentiation (online supplemental figure 5).

Taken together, these data indicate that less bone destruction in ActβA$^{d/d}$ ColVI-Cre hTNFtg mice is caused by reduced OC formation due to less activin A secretion by FLS.

Deficiency of activin A in ColVI-Cre-expressing cells highly ameliorates inflammation and bone destruction in hTNFtg mice

Next, we investigated whether a deletion of activin A in mesenchymal cells via ColVI-Cre has an effect on arthritis severity in vivo. To this end, ActβA$^{d/d}$ ColVI-Cre mice were cross-bred with hTNFtg mice to generate conditional deleted arthritic mice. Again, no significant differences in the clinical scores between ActβA$^{f/f}$ hTNFtg and ActβA$^{d/d}$ ColVI-Cre hTNFtg mice was observed. As expected, ActβA$^{f/f}$ and ActβA$^{d/d}$ ColVI-Cre showed no signs of arthritis (figure 6A,B). Evaluation of serum confirmed significantly reduced activin A levels by about 68% in mice with SF-specific activin A deletion compared with non-deleted arthritic mice (online supplemental figure 3A).

Most importantly, µCT and histomorphometry at the age of 12 weeks (figure 6C–E), as well as its quantitative assessment demonstrated a strong reduction of inflammation displayed by less formation of pannus tissue (46.3 %) and a distinct reduction of bone erosion (33.8 %) associated with a significant reduction in the number of OCs (46.2 %) in ActβA$^{d/d}$ ColVI-Cre hTNFtg mice compared with ActβA$^{f/f}$ hTNFtg mice (figure 6F–H and online supplemental figure 6). In consideration of the fact that activin A also stimulates the production of central players in inflammation such as IL-1 and IL-6,[28 30] corresponding serum levels in activin A-deleted and non-deleted arthritic mice were assessed. Indeed, deletion of activin A caused a strong reduction in IL-1 and IL-6 serum levels (51.7% and 47.5%, respectively), confirming an anti-inflammatory effect of activin A via the downregulation of proinflammatory cytokines (online supplemental figure 3B). Assuming that a deletion of activin A in ColVI-Cre-expressing cells within the joint will mainly led to a deletion in FLS, the results strongly indicate that FLS-derived activin A

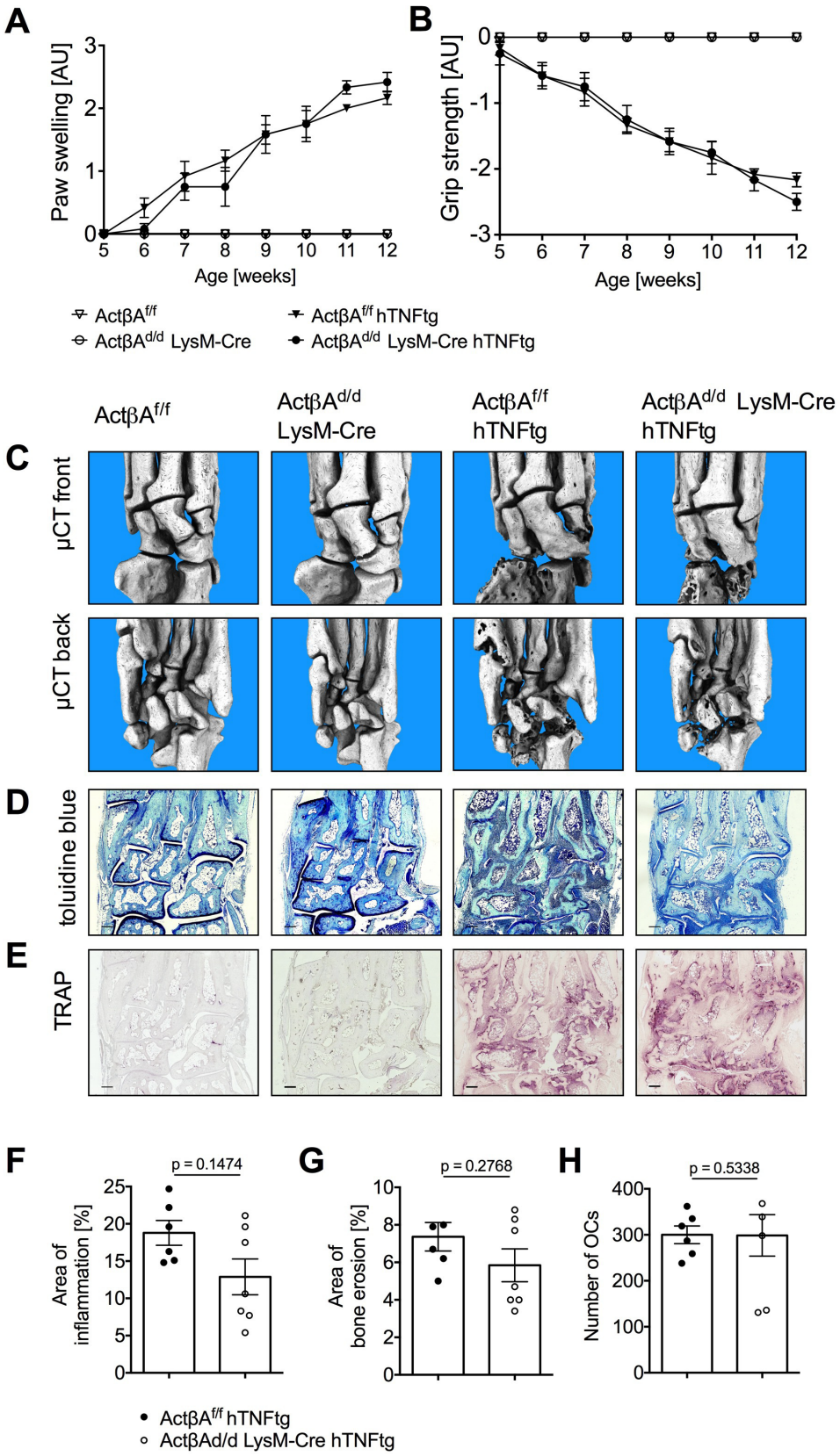

Figure 4 Deficiency of activin A in LysM-Cre-expressing cells does not substantially affect disease severity in hTNFtg mice. (A) Paw swelling and (B) grip strength measured in ActβA$^{f/f}$ (n=6), ActβA$^{d/d}$ LysM-Cre (n=6), ActβA$^{f/f}$ hTNFtg (n=6) and ActβA$^{d/d}$ LysM-Cre hTNFtg (n=6) mice over 5–12 weeks. All data are means±SEM (two-way analysis of variance, Bonferroni's multiple comparison test). (C) Representative images of µCT analysis from the front and back (n=4, each genotype), (D) toluidine blue-stained sections (scale bar 200 µm) and (E) TRAP-stained sections (scale bar 200 µm) from the hind paws of 12-week-old ActβA$^{f/f}$ (n=3), ActβA$^{d/d}$ LysM-Cre (n=3), ActβA$^{f/f}$ hTNFtg (n=6) and ActβA$^{d/d}$ LysM-Cre hTNFtg (n=7) mice. Quantitative histomorphometric assessment of (F) synovial pannus formation, (G) bone erosion and (H) number of OCs in tarsal joints. All data are means±SEM (Mann-Whitney U test). µCT, micro-CT; ActβA$^{f/f}$, ActβA$^{flox/flox}$; OC, osteoclast.

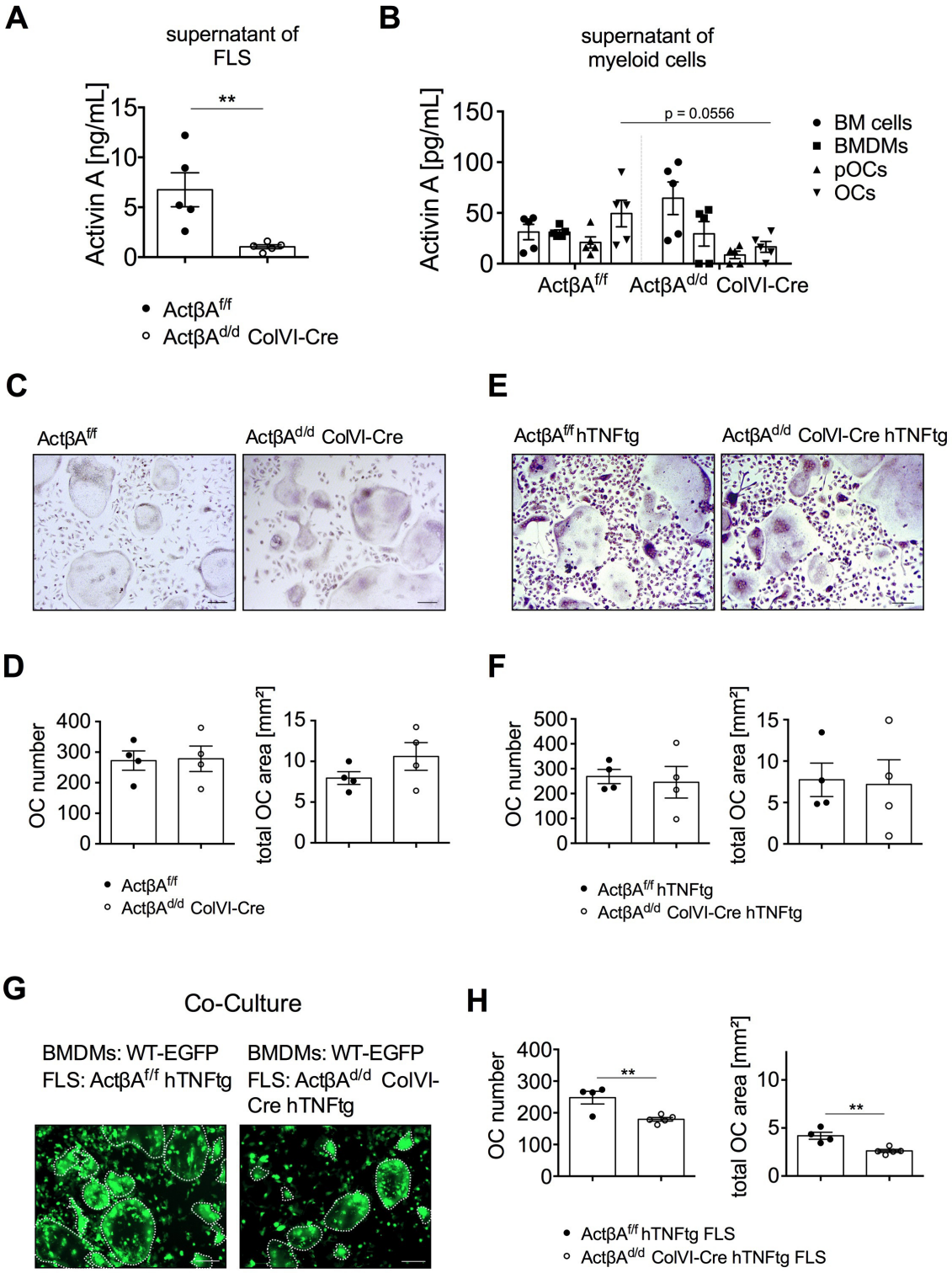

Figure 5 Deficiency of activin A in FLS significantly reduces OC formation. (A) Secretion of activin A by FLS from ActβA$^{f/f}$ and ActβA$^{d/d}$ ColVI-Cre mice after 48 hours. (B) Secretion of activin A by BM cells, BMDMs, pOCs and OCs from ActβA$^{f/f}$ and ActβA$^{d/d}$ ColVI-Cre mice after 48 hours. BM cells were not stimulated; BMDMs were stimulated with M-CSF (30 ng/mL) for 3 days; pOCs were stimulated for 3 days with M-CSF (30 ng/mL) followed by stimulation with M-CSF and RANKL (50 ng/mL) for a further 2 days. OCs were generated by stimulation of pOCs for a further 2 days with RANKL. All data are means±SEM (n=3–5, Mann-Whitney U test**). (C) Representative images of TRAP staining after 5 days of differentiation of BMDMs from ActβA$^{f/f}$ and ActβA$^{d/d}$ ColVI-Cre mice (scale bar 100 µm). (D) Corresponding OC number and total OC area per well. All data are means±SEM (n=4, Mann-Whitney U test). (E) Representative images of TRAP staining after 5 days of differentiation of BMDMs from ActβA$^{f/f}$ hTNFtg and ActβA$^{d/d}$ LysM-Cre hTNFtg mice (scale bar 100 µm). (F) Corresponding OC number and total OC area per well. All data are means±SEM (n=4, Mann-Whitney U test). (G) Representative fluorescence images of WT-EGFP BMDMs cocultured with FLS from ActβA$^{f/f}$ hTNFtg and ActβA$^{d/d}$ ColVI-Cre hTNFtg mice for 5 days to induce OC differentiation in presence of 1 µM PGE_2 (scale bar 100 µm). (H) Corresponding OC number and total OC area per well. All data are means±SEM (ActβA$^{f/f}$ hTNFtg n=4, ActβA$^{d/d}$ ColVI-Cre hTNFtg n=5, unpaired t-test**). **P≤0.01. FLS, fibroblast-like synoviocytes; OC, osteoclast; RANKL, receptor activator of nuclear factor κB ligand.

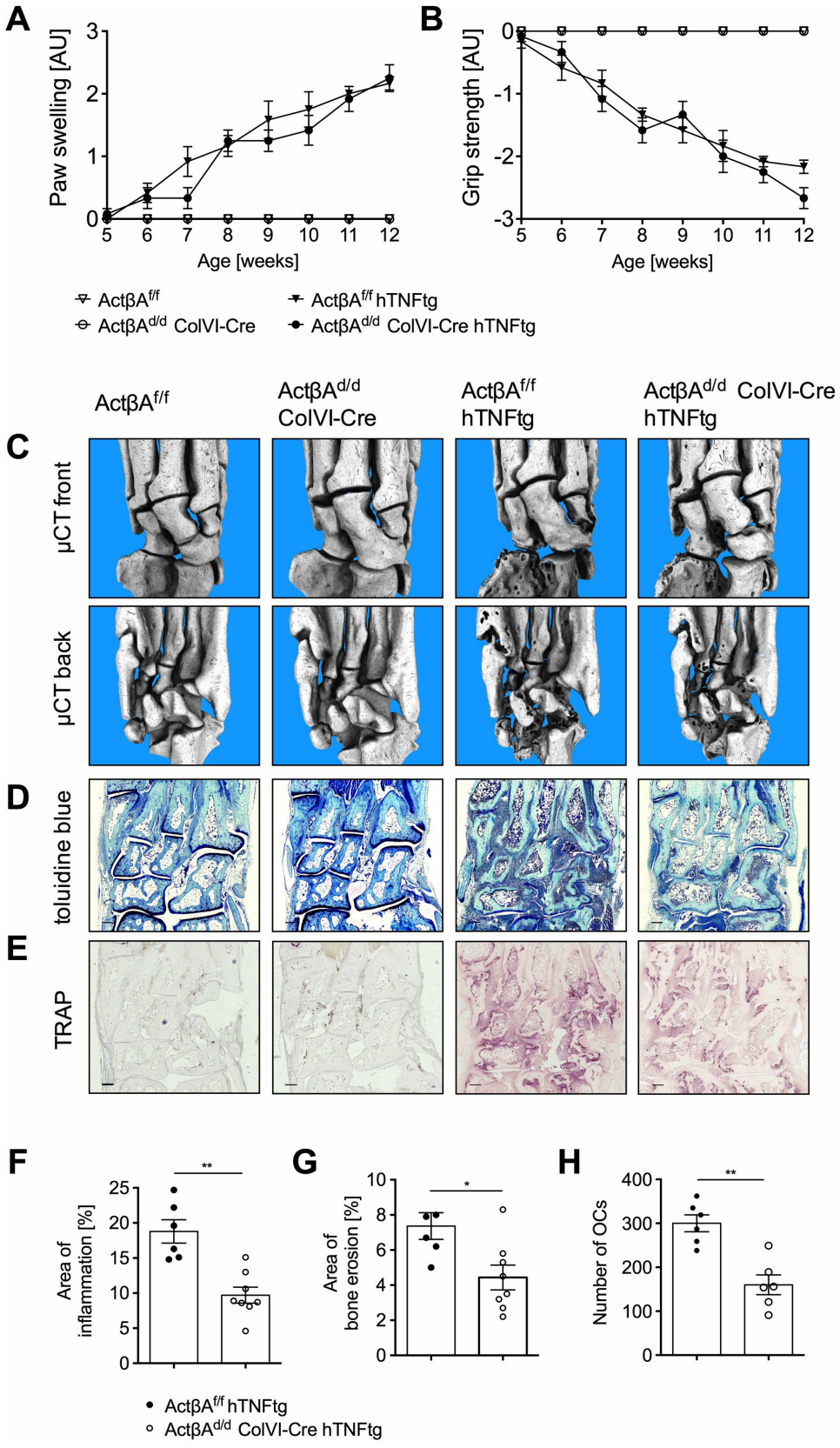

Figure 6 Deficiency of activin A in ColVI-Cre-expressing cells ameliorates disease severity in hTNFtg mice. (A) Paw swelling and (B) grip strength measured in ActβA$^{f/f}$ (n=6), ActβA$^{d/d}$ ColVI-Cre (n=6), ActβA$^{f/f}$ hTNFtg (n=6) and ActβA$^{d/d}$ ColVI-Cre hTNFtg (n=6) mice over 5–12 weeks. All data are means±SEM (two-way analysis of variance, Bonferroni's multiple comparison test). (C) Representative images of µCT analysis from the front and back (n=4, each genotype), (D) Toluidine blue-stained sections (scale bar 200 µm) and (E) TRAP-stained sections (scale bar 200 µm) from the hind paws of 12-week-old ActβA$^{f/f}$ (n=3), ActβA$^{d/d}$ ColVI-Cre (n=3), ActβA$^{f/f}$ hTNFtg (n=6) and ActβA$^{d/d}$ ColVI-Cre hTNFtg (n=6–8) mice. Quantitative histomorphometric assessment of (F) synovial pannus formation, (G) bone erosion and (H) number of OCs in tarsal joints. All data are means±SEM (Mann-Whitney U test). *P≤0.05, **P≤0.01. µCT, micro-CT; OC, osteoclast.

plays an important role in hTNFα-driven RA-like pathogenesis in mice.

Activin A enhances expression of key differentiation genes via Smad2-dependent nuclear translocation of NFATc1

To shed light on the mechanisms by which activin A exerts its effect on OC formation, we focused on potential signalling pathways and the expression of the key markers for OC differentiation.

Western Blot analysis of P-JNK, P-ERK and P-p38 demonstrated that RANKL, but not activin A, induces MAP kinase activation (figure 7A), phosphorylation of NF-κB and degradation of IκBα (figure 7B), indicating that the stimulatory effect of activin A on osteoclastogenesis did not originate from increased MAP kinase and nuclear factor kappa B (NF-κB) signalling. In consideration of the fact that TGF-β-like proteins activate the Smad2/3 signalling pathway, the ability of activin A to activate Smad2 in primary BMDMs was verified. Activin A induced Smad2 phosphorylation after 30 min, while RANKL had no effect on Smad2 activation (figure 7C). Of note, Smad2 phosphorylation was still present on stimulation with activin A for 3 and 4 days (figure 7D). Due to the enhanced osteoclastogenesis associated with activated Smad2 signalling by activin A, it was speculated that activated Smad2 may interact with the key transcription factor in OC differentiation NFATc1, which then could enhance the expression of a set of genes that are essential for osteoclastogenesis. To demonstrate that Smad2 and NFATc1 interact on stimulation with RANKL and activin A, coimmunoprecipitation experiments were performed. As shown in figure 7E, NFATc1 was clearly bound to P-Smad2 on costimulation of BMDMs with RANKL and activin A. Subsequent analyses of the key differentiation makers integrin αv, integrin β3, DC-STAMP, NFATc1 and cathepsin K showed that RANKL induced the expression of all these differentiation markers, whereas activin A alone did not induce any of these marker genes. However, activin A was clearly able to enhance the RANKL-induced expression of all differentiation markers during osteoclastogenesis (figure 7F).

In order to verify whether the stimulatory effect of activin A on OC formation exclusively depends on receptor-mediated Smad2 signalling, a specific ALK4/5/7 inhibitor (SB431542) was used during OC differentiation. TRAP staining showed that treatment with ALK4/5/7 inhibitor strongly reduced the activin A-enhanced OC formation (figure 7G). Quantification revealed a strong inhibition of osteoclastogenesis either on stimulation with RANKL plus activin A compared with untreated differentiation controls, confirming a receptor-mediated and Smad-dependent impact of activin A on OC formation. Finally, recovery experiments showed that the inhibitor was not toxic and OC differentiation increased again after withdrawal of the inhibitor (figure 7H). However, OC differentiation was already reduced on stimulation with RANKL alone, assuming additional autocrine factors. Beside activin A, OC precursors also express myostatin, which similar to activin promotes OC differentiation by activating the Smad pathway. Since both myostatin and activin A signal through a combination of Acvr2b and/or Acvr2a and ALK4/5 or ALK4/7 activating the Smad pathway, the ALK inhibitor will block both the activin and the myostatin-induced Smad2 activation, which very likely cause the inhibition of basal RANKL-induced OC development.

Together, these results led to the conclusion that the stimulating effect of activin A on osteoclastogenesis is mediated by the interaction of P-Smad2 and the key transcription factor of osteoclastogenesis NFATc1, thereby enhancing the expression of osteoclastic genes and subsequently OC development.

DISCUSSION

RA is common type of inflammatory arthritis characterised by chronic inflammation, culminating in joint damage due to cartilage and bone destruction. Identification of molecules and associated signalling pathways involved in these destructive processes has become increasingly important. A family of proteins that affects inflammatory processes and bone metabolism is the TGF-β superfamily, under which activin A has found to be markedly elevated in serum, synovial fluid and synovial tissue of patients with RA[25–28] and to stimulate the production of inflammatory mediators.[29 30] Moreover, activin A is expressed in cells that are involved in bone metabolism such as BM cells, macrophages, OCs and OBs,[26 29 38–42] as well as in FLS that are abundantly present in the inflamed synovium of patients with RA,[1 26 28 43] all suggesting a role of activin A in inflammatory bone remodelling. In accordance with this, we observed highly elevated levels of activin A in synovial tissues obtained from patients with RA as well as from arthritic mice, suggesting that the inflammatory environment leads to an upregulation of activin A expression. Interestingly, in patients with RA, activin A-expressing cells were mostly found in the synovial sublining layer, indicating that within the synovial tissue, FLS are the main producer of activin A.

In more detail, stimulation of FLS and BMDMs with proinflammatory cytokines showed that activin A secretion by FLS was increased on stimulation with proinflammatory cytokines, while activin A secretion by BMDMs was not affected. In addition, activin A secretion by FLS was considerably higher than by BMDMs and even still higher in arthritic FLS compared with WT FLS.

Intriguingly, IL-17A strongly enhanced activin A secretion in hTNFtg but not in WT FLS. In this regard, former studies could show that IL-17-RA and IL-17RC are overexpressed in peripheral whole blood obtained from patients with RA, and these receptors are also highly expressed in the synovium of patients with RA, as well as by RA-FLS,[44 45] probably explaining why arthritic FLS were more susceptible to IL-17A stimulation than WT FLS.

Altogether, these data strongly support the hypothesis that FLS-derived activin A may be an important regulator of inflammatory arthritis.

Since inflammation-induced bone destruction is one main feature of RA, we evaluated the contribution of activin A to OC differentiation in vitro and bone erosion in vivo. Indeed, activin A strongly increased RANKL-induced OC formation and resorptive activity in vitro, which is in line with others.[14–19] Moreover, enhancement of osteoclastogenesis was mediated by the induction of Smad2 phosphorylation, which is consistent with studies from Murase *et al* and Kajita *et al*.[15 19] However, this study showed for the first time that stimulation of primary BMDMs with activin A and RANKL led to an interaction of phospho-Smad2 with NFATc1, the key transcription factor of OC differentiation. Taking additionally the activin A-induced increase of OC differentiation and activity markers into account, we hypothesise that interaction of NFATc1 with phospho-Smad2 led to an increased translocation of NFATc1 into the nucleus, thereby enhancing the expression of OC-specific genes. Since this interaction has also been observed in myostatin-enhanced osteoclastogenesis, it seems to be a common mechanism by which members of the TGF-β family can regulate OC formation.[37]

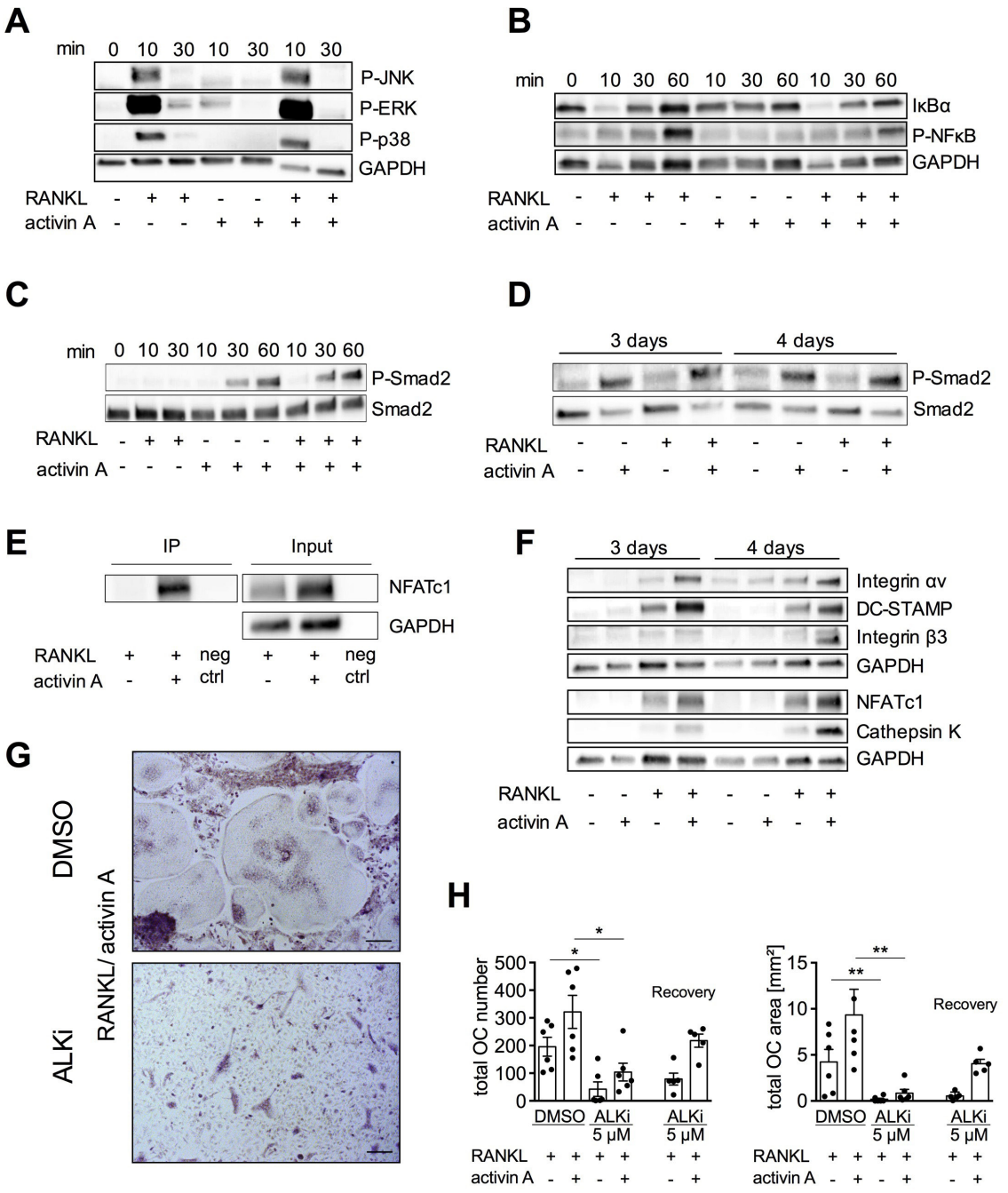

Figure 7 Activin A enhances RANKL-mediated OC formation and expression of OC differentiation markers by activation of Smad2. (A) Representative immunoblots of p-JNK, P-ERK and P-p38 of WT BMDMs stimulated with RANKL (50 ng/mL), activin A (30 ng/mL) or RANKL plus activin A in the presence of M-CSF (30 ng/mL) for 10 and 30 min. Unstimulated BMDMs served as control and glycerinaldehyde-3-phosphate dehydrogenase (GAPDH) as loading control (n=3). (B) Representative immunoblots of IκBα and NF-κB on stimulation of WT BMDMs with RANKL (50 ng/mL), activin A (30 ng/mL) or RANKL plus activin A for 10, 30 and 60 min always in the presence of M-CSF (30 ng/mL). Unstimulated BMDMs were used as control and GAPDH as loading control (n=3). (C) Representative immunoblots of P-Smad2 and Smad2 after stimulation of BMDMs with RANKL (50 ng/mL), activin A (30 ng/mL) or RANKL plus activin A for 10, 30 and 60 min (n=3) and (D) after 3 and 4 days (n=3). (E) Representative immunoblots of coimmunoprecipitation analyses. P-Smad2, coupled to protein G-labelled Dynabeads, was incubated equal amounts of protein lysates of BMDMs stimulated with RANKL, or RANKL plus activin A for 2 days was transferred to the antibody-bead complex. After incubation, pulldown was performed followed by western blot analysis against NFATc1 of the coimmunoprecipitated protein and equal amounts of the total protein lysates (input). Lysis buffer was used as negative control (neg ctrl) (n=3). (F) representative immunoblots of the OC differentiation markers integrin αv, integrin β3, DC-STAMP, NFATc1 and cathepsin K on stimulation of WT BMDMs with activin A (30 ng/mL), RANKL (50 ng/mL) or RANKL plus activin A for 3 and 4 days always in the presence of M-CSF (30 ng/mL). Unstimulated BMDMs served as control. GAPDH was used as loading control (n=3). (G) Representative images of TRAP staining after 4 days of differentiation. (H) Quantification of OC number and area on treatment of BMDMs with an ALK4/5/7 inhibitor together with RANKL (50 ng/mL) or RANKL plus activin A (30 ng/mL) for 4 days. For recovery experiments, ALK4/5/7 inhibitor was removed and BMDMs were stimulated with RANKL or RANKL plus activin A for a further 2 days. The ALK4/5/7 inhibitor was diluted in DMSO; therefore, DMSO-treated BMDMs served as control. All data are means±SEM (n=5–6, Mann-Whitney U test). All experiments were performed in the presence of M-CSF (30 ng/mL). *P≤0.05, **P≤0.01. OC, osteoclast; RANKL, receptor activator of nuclear factor κB ligand.

Therefore, the interaction domains of phospho-Smad2 and NFATc1 might by interesting targets for the treatment of diseases with OC-mediated bone loss such as RA or osteoporosis. Finally, the fact that activin A also stimulates human OC differentiation further confirms the importance of activin A as an osteoclastogenic factor.

Based on the observation that activin A is upregulated within an inflammatory environment, we wondered whether the loss of activin A protects against bone damage during inflammatory destructive arthritis. Since FLS and macrophages appeared to be the main activin A-expressing cells within the inflamed synovium, we assessed the effect of activin A deficiency in ColVI-Cre-expressing and LysM-Cre-expressing cells on disease severity in the hTNFtg mouse model of arthritis.

The deficiency of activin A in myeloid cells (LysM-Cre) does not significantly affect inflammation, bone erosion and OC numbers in hind paws of hTNFtg mice, although a tendency towards a reduced inflammation was observed. The missing impact of this cell-specific deletion on OC formation and bone erosion is probably due to the very small amounts of activin A produced by myeloid cells compared with FLS (pg vs ng range). This assumption is further supported by the fact that the lack of autocrine activin A in BM cells, BMDMs, pOCs and OCs from $Act\beta A^{d/d}$ LysM-Cre or $Act\beta A^{d/d}$ LysM-Cre hTNFtg mice does not affect OC development.

In contrast, although the clinical scores were not affected by the loss of activin A, histomorphometric analyses clearly showed that deficiency of activin A in ColVI-Cre-expressing cells such as FLS strongly reduces OC formation (about 47%) in the hTNFtg model and thereby attenuating bone erosion (about 40%). These results highly suggest that paracrine, but not autocrine activin A, is important for inflammation-mediated bone erosion by directly acting on OC precursors and thereby regulating OC differentiation and activity. Results from coculture experiments demonstrating that the cell-specific deletion of activin A in FLS leads to less OC differentiation further substantiate the major role of paracrine activin A. However, additional in vivo studies would be helpful to further clarify the relative contribution of FLS-derived myostatin and activin A to OC differentiation in RA.

Moreover, serum levels of proinflammatory cytokines were highly reduced (about 50%), and pannus formation, which also reflects the degree of joint inflammation, was strongly reduced about 48% as well on lack of activin A, both confirming an anti-inflammatory effect of activin A deletion. In this context, activin A was shown to induce cell proliferation of RA-FLS,[26] which potentially may contribute to the formation of pannus tissue within the inflammatory environment. Moreover, it is well known that FLS within the pannus tissue are activated by their proinflammatory environment, resulting in an aggressive phenotype that is maintained even in the absence of inflammatory stimuli.[3 4 46] In this context, activated FLS produce inflammatory cytokines, chemokines, growth factors and degrading enzymes, thereby regulating joint inflammation and destruction. The fact that FLS appeared the be the main producers of activin A in the joint and that the lack of FLS-derived activin A exceedingly ameliorates disease severity confirm the prominent role of FLS in arthritis.

In conclusion, we could show for the first time that activin A significantly regulates disease severity in a mouse model of chronic arthritis. Deletion of paracrine but not autocrine activin A reduces OC formation and bone destruction and most interestingly reduces also joint inflammation in our arthritis model. Thus, inhibition of activin A may be a promising treatment option for arthritis and other diseases associated with inflammatory bone loss.

Correction notice This article has been corrected since it was first published. The open access licence has been updated to CC BY.

Acknowledgements ActβAflox/flox mice were kindly provided by M Matzuk (Baylor College of Medicine, Houston, USA); ColVI-Cre and hTNFtg mice (strain Tg197) were provided by G Kollias (Alexander Fleming Biomedical Sciences Research Center, Vari, Greece).

Contributors BD and TP conceived the study. VW-K performed most of the experiments. EW, MF, JI, CW and PP were involved in the mouse studies, including histological and micro-CT analyses. DB and JR performed the fluorescence stainings. JR and MD performed the human osteoclast experiments. AK-P and CW participated in data discussion and interpretation. VW-K, BD and TP drafted the manuscript. All authors read, commented on and approved the final manuscript. BD acts as guarantor.

Funding This work was supported by the German Research Foundation (Deutsche Forschungsgemeinschaft) as part of the Collaborative Research Center SFB 1009 both granted to BD and TP.

Competing interests None declared.

Patient and public involvement Patients and/or the public were not involved in the design, conduct, reporting or dissemination plans of this research.

Patient consent for publication Not applicable.

Ethics approval Human synovial tissue samples were obtained from patients with a clinical diagnosis of rheumatoid arthritis after informed consent prior to surgery (ethics committee of the Medical Faculty of the Westfalian Wilhelms-University Muenster (2009-447-f-S)). Animal experimental protocols were approved by the Animal Welfare and Ethical Review Committee 'Landesamt für Natur, Umwelt und Verbraucherschutz Nordrhein-Westfalen' (84.02.04.2017. A112).

Provenance and peer review Not commissioned; externally peer reviewed.

Data availability statement All data relevant to the study are included in the article. All study data are included in the article and supporting information.

ORCID iD

Berno Dankbar http://orcid.org/0000-0002-7893-1417

REFERENCES

1 Smolen JS, Steiner G. Therapeutic strategies for rheumatoid arthritis. *Nat Rev Drug Discov* 2003;2:473–88.
2 Edwards JC, Willoughby DA. Demonstration of bone marrow derived cells in synovial lining by means of giant intracellular granules as genetic markers. *Ann Rheum Dis* 1982;41:177–82.
3 Qu Z, Garcia CH, O'Rourke LM, *et al*. Local proliferation of fibroblast-like synoviocytes contributes to synovial hyperplasia. *Arthritis & Rheumatism* 1994;37:212–20.
4 Müller-Ladner U, Kriegsmann J, Franklin BN, *et al*. Synovial fibroblasts of patients with rheumatoid arthritis attach to and invade normal human cartilage when engrafted into SCID mice. *Am J Pathol* 1996;149:1607–15.
5 Huber LC, Distler O, Tarner I, *et al*. Synovial fibroblasts: key players in rheumatoid arthritis. *Rheumatology* 2006;45:669–75.
6 A. Hitchon C, El-Gabalawy HS. The synovium in rheumatoid arthritis. *Open Rheumatol J* 2011;5:107–14.
7 Gravallese EM, Harada Y, Wang JT, *et al*. Identification of cell types responsible for bone resorption in rheumatoid arthritis and juvenile rheumatoid arthritis. *Am J Pathol* 1998;152:943–51.
8 Bromley M, Evanson JM, Woolley DE. Chondroclasts and osteoclasts at subchondral sites of cartilage erosion in the rheumatoid joint. *Bone* 1986;7:146.

9 Georganas C, Liu H, Perlman H, *et al*. Regulation of IL-6 and IL-8 expression in rheumatoid arthritis synovial fibroblasts: the dominant role for NF-kappa B but not C/EBP beta or c-Jun. *J Immunol* 2000;165:7199–206.
10 Hashizume M, Hayakawa N, Mihara M. Il-6 trans-signalling directly induces RANKL on fibroblast-like synovial cells and is involved in RANKL induction by TNF-alpha and IL-17. *Rheumatology* 2008;47:1635–40.
11 Hofbauer LC, Lacey DL, Dunstan CR, *et al*. Interleukin-1Beta and tumor necrosis factor-alpha, but not interleukin-6, stimulate osteoprotegerin ligand gene expression in human osteoblastic cells. *Bone* 1999;25:255–9.
12 Kotake S, Udagawa N, Takahashi N, *et al*. Il-17 in synovial fluids from patients with rheumatoid arthritis is a potent stimulator of osteoclastogenesis. *J Clin Invest* 1999;103:1345–52.
13 Kotake S, Sato K, Kim KJ, *et al*. Interleukin-6 and soluble interleukin-6 receptors in the synovial fluids from rheumatoid arthritis patients are responsible for osteoclast-like cell formation. *J Bone Miner Res* 1996;11:88–95.
14 Fuller K, Bayley KE, Chambers TJ. Activin A is an essential cofactor for osteoclast induction. *Biochem Biophys Res Commun* 2000;268:2–7.
15 Murase Y, Okahashi N, Koseki T, *et al*. Possible involvement of protein kinases and Smad2 signaling pathways on osteoclast differentiation enhanced by activin a. *J Cell Physiol* 2001;188:236–42.
16 Sakai R, Eto Y, Ohtsuka M, *et al*. Activin enhances osteoclast-like cell formation in vitro. *Biochem Biophys Res Commun* 1993;195:39–46.
17 Sugatani T, Alvarez UM, Hruska KA. Activin A stimulates IkappaB-alpha/NFkappaB and RANK expression for osteoclast differentiation, but not Akt survival pathway in osteoclast precursors. *J Cell Biochem* 2003;90:59–67.
18 Gaddy-Kurten D, Coker JK, Abe E, *et al*. Inhibin suppresses and activin stimulates osteoblastogenesis and osteoclastogenesis in murine bone marrow cultures. *Endocrinology* 2002;143:74–83.
19 Kajita T, Ariyoshi W, Okinaga T, *et al*. Mechanisms involved in enhancement of osteoclast formation by activin-A. *J Cell Biochem* 2018;119:6974–85.
20 Mason AJ, Hayflick JS, Ling N, *et al*. Complementary DNA sequences of ovarian follicular fluid inhibin show precursor structure and homology with transforming growth factor-beta. *Nature* 1985;318:659–63.
21 Nakamura T, Asashima M, Eto Y, *et al*. Isolation and characterization of native activin B. *J Biol Chem* 1992;267:16385–9.
22 Fukui A, Nakamura T, Sugino K, *et al*. Isolation and characterization of Xenopus follistatin and activins. *Dev Biol* 1993;159:131–9.
23 McInnes IB, Schett G. Cytokines in the pathogenesis of rheumatoid arthritis. *Nat Rev Immunol* 2007;7:429–42.
24 Turner MD, Nedjai B, Hurst T, *et al*. Cytokines and chemokines: at the crossroads of cell signalling and inflammatory disease. *Biochim Biophys Acta* 2014;1843:2563–82.
25 Gribi R, Tanaka T, Harper-Summers R, *et al*. Expression of activin A in inflammatory arthropathies. *Mol Cell Endocrinol* 2001;180:163–7.
26 Ota F, Maeshima A, Yamashita S, *et al*. Activin A induces cell proliferation of fibroblast-like synoviocytes in rheumatoid arthritis. *Arthritis Rheum* 2003;48:2442–9.
27 El-Gendi SS, Moniem AEA, Tawfik NM, *et al*. Value of serum and synovial fluid activin A and inhibin A in some rheumatic diseases. *Int J Rheum Dis* 2010;13:273–9.
28 Diller M, Frommer K, Dankbar B, *et al*. The activin-follistatin anti-inflammatory cycle is deregulated in synovial fibroblasts. *Arthritis Res Ther* 2019;21:1–11.
29 Sierra-Filardi E, Puig-Kröger A, Blanco FJ, *et al*. Activin a skews macrophage polarization by promoting a proinflammatory phenotype and inhibiting the acquisition of anti-inflammatory macrophage markers. *Blood* 2011;117:5092–101.
30 Yamashita N, Nakajima T, Takahashi H, *et al*. Effects of activin A on IgE synthesis and cytokine production by human peripheral mononuclear cells. *Clin Exp Immunol* 1993;94:214–9.
31 Nüsing RM, Barsig J. Induction of prostanoid, nitric oxide, and cytokine formation in rat bone marrow derived macrophages by activin a. *Br J Pharmacol* 1999;127:919–26.
32 Matzuk MM, Kumar TR, Vassalli A, *et al*. Functional analysis of activins during mammalian development. *Nature* 1995;374:354–6.
33 Clausen BE, Burkhardt C, Reith W, *et al*. Conditional gene targeting in macrophages and granulocytes using LysMcre mice. *Transgenic Res* 1999;8:265–77.
34 Pangas SA, Jorgez CJ, Tran M, *et al*. Intraovarian activins are required for female fertility. *Mol Endocrinol* 2007;21:2458–71.
35 Keffer J, Probert L, Cazlaris H, *et al*. Transgenic mice expressing human tumour necrosis factor: a predictive genetic model of arthritis. *Embo J* 1991;10:4025–31.
36 Armaka M, Apostolaki M, Jacques P, *et al*. Mesenchymal cell targeting by TNF as a common pathogenic principle in chronic inflammatory joint and intestinal diseases. *J Exp Med* 2008;205:331–7.
37 Dankbar B, Fennen M, Brunert D, *et al*. Myostatin is a direct regulator of osteoclast differentiation and its inhibition reduces inflammatory joint destruction in mice. *Nat Med* 2015;21:1085–90.
38 Eijken M, Swagemakers S, Koedam M, *et al*. The activin A-follistatin system: potent regulator of human extracellular matrix mineralization. *Faseb J* 2007;21:2949–60.
39 Hosoi T, Inoue S, Hoshino S, *et al*. Immunohistochemical detection of activin A in osteoclasts. *Gerontology* 1996;42:20–4.
40 Ikenoue T, Jingushi S, Urabe K, *et al*. Inhibitory effects of activin-A on osteoblast differentiation during cultures of fetal rat calvarial cells. *J Cell Biochem* 1999;75:206–14.
41 Meunier H, Rivier C, Evans RM, *et al*. Gonadal and extragonadal expression of inhibin alpha, beta A, and beta B subunits in various tissues predicts diverse functions. *Proc Natl Acad Sci U S A* 1988;85:247–51.
42 Yu AW, Shao LE, Frigon NL, *et al*. Detection of functional and dimeric activin A in human marrow microenvironment. Implications for the modulation of erythropoiesis. *Ann N Y Acad Sci* 1994;718:285–99.
43 Barland P, Novikoff AB, Hamerman D. Electron microscopy of the human synovial membrane. *J Cell Biol* 1962;14:207–20.
44 Kehlen A, Thiele K, Riemann D, *et al*. Expression, modulation and signalling of IL-17 receptor in fibroblast-like synoviocytes of patients with rheumatoid arthritis. *Clin Exp Immunol* 2002;127:539–46.
45 Zrioual S, Toh M-L, Tournadre A, *et al*. IL-17RA and IL-17RC receptors are essential for IL-17A-induced ELR+ CXC chemokine expression in synoviocytes and are overexpressed in rheumatoid blood. *J Immunol* 2008;180:655–63.
46 Ospelt C, Reedquist KA, Gay S, *et al*. Inflammatory memories: is epigenetics the missing link to persistent stromal cell activation in rheumatoid arthritis? *Autoimmun Rev* 2011;10:519–24.

Deletion of activin A in mesenchymal but not myeloid cells ameliorates disease severity in experimental arthritis

Vanessa Waltereit-Kracke[1], Corinna Wehmeyer[1], Denise Beckmann[1], Eugenie Werbenko[1], Julia Reinhardt[1], Fabienne Geers[1], Mike Dienstbier[1], Michelle Fennen[1], Johanna Intemann[1], Peter Paruzel[1], Adelheid Korb-Pap[1], Thomas Pap[1], Berno Dankbar[1]

[1]WWU Muenster, Institute of Musculoskeletal Medicine (IMM), Muenster, Germany

Corresponding author (to whom also reprint requests should be sent):
Berno Dankbar, PhD
Institute of Musculoskeletal Medicine
University Hospital Muenster
Albert-Schweitzer-Campus 1, Bldg. D3
D-48149 Muenster
Germany
Phone: +49-251-835 6756
Fax: +49-251-835 7462
Email: dankbarb@uni-muenster.de

Supplemental material

Methods

Human synovial tissues and cells. All studies with human samples were approved by the ethics committee of University Hospital Münster. Synovial tissues from patients with RA or OA (according to the 1987 revised American College of Rheumatology criteria for RA and OA) were obtained during joint replacement surgery (Department of Orthopaedic Surgery, St. Joseph Hospital, Sendenhorst, Germany; Department of Orthopeadic Surgery of the University of Magdeburg School of Medicine, Magdeburg, Germany; Department of Orthopeadic Surgery, KMG-Kliniken Kyritz, Germany). All patients submitted informed consent prior to surgery. Human synovial fibroblasts were isolated by enzymatic digestion of synovial tissues using dispase II, cultured in DMEM with 10 % FCS and were used between passages 4 and 7. Human peripheral blood mononuclear cells (PBMC) were isolated from peripheral blood using Histopaque-1077 (Merck, Darmstadt, Germany) according to the manufacturer's instructions.

Animals. Actβ$A^{flox/flox}$, LysM-Cre (provided by University Hospital, Münster, Germany) and ColVI-Cre mice have been described previously[32–34]. Actβ$A^{flox/flox}$ mice were mated with Cre mice in order to obtain Actβ$A^{d/d}$ LysM-Cre and Actβ$A^{d/d}$ ColVI-Cre mice. These mice were then crossbred with hTNFtg mice (strain Tg197[35]) to obtain arthritic mice with cell-specific deletions of activin A. Mice were sacrificed at the age of 12 weeks. All mouse strains were kept at the C57BL/6J genetic background. Standard animal husbandry in accordance with the institutional guidelines was performed to generate cohorts of male and female mice. All animal procedures have been approved by the local ethics committee „Landesamt für Natur, Umwelt und Verbraucherschutz

Nordrhein-Westfalen“ (LANUV; 84.02.04.2017.A112) and were carried out in compliance with the ARRIVE guidelines.

Immunofluorescence staining. Human and murine tissue samples were fixed in 4 % paraformaldehyde overnight, embedded in paraffin and cut into 5 µm sections. Murine hind paws were additionally decalcified in ammonium EDTA before embedding in paraffin. Deparaffinized sections were rehydrated and antigen retrieval was performed with 1x Trypsin/EDTA (PAA Laboratories, Pasching, Austria) in a humid chamber for 10 minutes at 37°C or incubated with citrate buffer (pH 2,5) in a humid chamber for 2 hours at RT. After digestion, the samples were washed with TBS. Afterwards the tissues were blocked in 10% horse serum for an hour. Sections were stained with primary antibodies, goat polyclonal to Activin A (R&D #AF338, dilution 1:50), mouse monoclonal to CD68 (Abcam #ab955, dilution 1:100), rabbit monoclonal to Myeloperoxidase (Abcam #ab208670, dilution 1:200) or rabbit polyclonal to Thy1/CD90 (LSBio #LS-C414760, dilution 1:100) overnight by 4°C. After washing with TBS, slices were incubated with secondary antibodies anti-goat 488 (Invitrogen #A-11055, dilution 1:5000), anti-mouse 555 (Invitrogen #A-31570, dilution 1:5000) and anti-rabbit 647 (Invitrogen #A-21245, dilution 1:5000) for an hour, counterstained with DAPI (Invitrogen #D1306, dilution 1:10.000) and mounted in aqueous mounting media.

Murine fibroblasts and bone marrow cells. Murine FLS were isolated from deskinned hind paws of 12-week old mice by enzymatic digestion with collagenase type IV (Worthington-Biochemical Corporation, Lakewood, USA) and cultured in DMEM with 10 % FCS at 37 °C and 5 % CO_2. To avoid contamination with other cells, passages 3 to 5 were used for further experiments. Murine bone marrow cells (BMCs) were isolated from femora and tibiae from 6- to 12-week old mice by flushing out BM

cells of the marrow cavity and cultivating them in α-MEM with 10 % FCS and 30 ng/mL M-CSF (R&D Systems, Nordenstadt, Germany) at 37 °C and 5 % CO_2 in order to differentiate them to BMDMs.

ELISA measurements. Concentrations of activin A, interleukin-1 alpha (mIL-1α) and interleukin-6 (mIL-6) in mouse serum and/or supernatants of stimulated and unstimulated FLS and BMDMs were analysed by Quantikine ELISA Kits (R&D Systems, Minneapolis, USA). All assays were performed according to the manufacturer's instructions.

Semi-quantitative PCR. Total RNA from human RA and hTNFtg FLS was isolated using peqGOLD TriFast™ (VWR, Radnor, USA) according to the manufacturer's instructions. Synthesis of cDNA was performed by using the iSkript™ cDNA Synthesis Kit (Bio-Rad Laboratories, Inc., Hercules, USA). The synthesized cDNA was used for PCR using human inhibin βA primers (forward CAT CAC GTT TGC CGA GTC AG, reverse GAC TGC TCC TTT TCC TCA TC) and GAPDH primers (forward TCC TGC ACC ACC AAC TGC TT, reverse TCC ACC ACC CTG TTG CTG TA) or the murine inhibin βA (forward GGG ACC CGA AAG AGA ATT TGC, reverse TCC TCT CAG CCA AAG CAA GG) and GAPDH primers (forward ATG TGT CCG TCG TGG ATC TG, reverse ATG TGT CCG TCG TGG ATC TG).

***In vitro* osteoclast generation and resorption assay.** Murine BMCs and human PBMCs were primed for 72 h with 30 ng/mL M-CSF (R&D Systems, Minneapolis, USA) followed by stimulation with 30 ng/mL M-CSF and 50 ng/mL RANKL (R&D Systems, Minneapolis, USA) for further 4 to 6 days (murine) or 15 days (human). To analyse the impact of activin A on OC formation 30 ng/mL or 100 ng/mL activin A (R&D Systems,

Minneapolis, USA) was added to WT BMDMs or PBMCs, respectively. Additionally, the impact of TGF-ß1 on OC formation was evaluated by incubation of WT BMDMs with 0.1 and 10 ng/mL TGF-ß1 (R&D Systems, Minneapolis, USA). To inhibit activin A-mediated receptor signaling, a specific ALK4/5/7 inhibitor (SB431542, Sigma-Aldrich, St. Louis, USA) with a concentration of 5 µM was used. To assess the toxicity of the inhibitor, recovery experiments were performed in which the inhibitor was removed, cells were washed with PBS and stimulated with 30 ng/mL M-CSF and 50 ng/mL RANKL with or without 30 ng/mL activin A. For inhibition experiments, cells were incubated with anti-activin A (0.3 µg/mL, R&D Systems) or anti-GDF-8 (3 µg/mL, R&D Systems) antibodies. OC formation was determined by TRAP staining (Acid Phosphatase, Leukocyte (TRAP) Kit, Sigma-Aldrich, St. Louis, USA).

Bone resorption assays were performed by seeding the cells on a calcium phosphate-coated 48-well plate followed by priming and stimulation as described for the OC differentiation. Afterwards, cells were removed by treating the wells with 5 % sodium hypochlorite and washed three times with PBS. For quantification of resorption pits, the entire wells were recorded with the Axio Observer Z1. The area of resorption pits was measured using ZEN 2 software.

Assessment of proliferation. For assessment of proliferation of BMDMs, cells were cultured with M-CSF (30 ng/mL) and with or without activin A (30 ng/mL) for 1, 2 and 3 days. Afterwards, cells were fixed with 4 % PFA for 15 min at RT, washed with PBS and stained for DAPI. The number of cells was determined by counting the DAPI stained cells in ImageJ.

Micro-CT and histomorphometric analysis. Hind paws of mice were fixed in 4 % PFA at 4 °C for 24 h and washed with PBS followed by scanning with Skyscan 1176

high resolution *in vivo* microtomograph (Bruker, Billerica, USA). The data were reconstructed by using NRecon v1.6.10.4 (Bruker, Billerica, USA) and exported as three-dimensional data by using CT Analyser v.1.16.4.1 (Bruker, Billerica, USA). The samples were shaded in MeshLab v2016.12 (Visual Computing Laboratory, Pisa, Italy) using ambient occlusion and snapshots were taken. For evaluation of trabecular and cortical bone parameters, images were reconstructed using the software NRecon v1.7.3.2 and analysed using the CTan v1.17.7.2.

Histomorphometric analysis was performed on toluidine-blue and TRAP stained paraffin sections. Images were taken of the tarsal joints of the hind paws using the Axio Observer Z1 microscope. Quantification was conducted with the ZEN software as described before [36]. Briefly, the area of inflammation was calculated on toluidine blue-stained sections as the sum of areas of inflamed tissue in tarsal joints in relation to the total tarsal joint area. To determine bone erosion, the area of bone loss was quantified on the same toluidine-blue stained section in relation to the total tarsal joint area. OCs were counted in TRAP-stained sections.

Co-Cultures. For co-cultures $5x10^3$ FLS were seeded in a 96-well containing FLS culture medium. On the next day, $1x10^5$ EGFP-BMCs were seeded onto the FLS layer and cultured for 3 - 6 days in OC medium containing 1 µM prostaglandin E_2 (PGE_2). OC differentiation was stopped by fixing the cells with 4 % PFA. For inhibition experiments, anti-activin A (0.3 µg/mL) and anti-myostatin (3 µg/mL) antibodies were applied (both R&D Systems). OC number was determined by visualizing the fixed cells by fluorescence using the Axio Observer Z1 and ZEN 2 software.

Co-immunoprecipitation. Co-Immunoprecipitation experiments were performed via Dynabeads™ Protein G according to the manufacturer's protocol. Phospho-Smad2

antibody was coupled to protein G-labelled Dynabeads. Equal amounts of cell lysates were transferred to the bead-bound antibody and incubated for 90 min at RT. Subsequent Western blot analysis against NFATc1 was performed.

Immunoblotting. Total protein lysates or co-immunoprecipitates were electrophoretically separated by 80 V for 1 - 2 h. Subsequent protein transfer to Trans-Blot® Turbo™ Mini PVDF membranes was carried out electrophoretically at 25 V for 3 min. PVDF membranes were blocked with BSA-based blocking solution for 1h at RT. The primary antibody was incubated overnight at 4 °C under continuous rotation. Afterwards, membranes were washed three times with TBS-T for 5 min followed by incubation with HRP-linked secondary antibody for 1h at RT under continuous rotation. Membranes were washed, incubated with ECL solution for 2 min, and protein of interest was visualized via chemiluminescence signaling using a Fusion FX Western blot imager.

Statistical analysis. All data are presented as means ± SEM or ± SD. Statistical analysis was performed using GraphPad Prism 7 software. Paired data were analysed by paired t-test, unpaired data were analysed by unpaired t-test or a Mann-Whitney-U test. If a t-test was used, the data were tested for normality using a D'Agostino & Person normality test or, in the case that the n-number was too small, a Shapiro-Wilk normality test was applied. In case of three or more groups, data were statistically analysed by ANOVA followed by Bonferroni's multiple comparison test. P-values ≤ 0.05 were considered as significant. * = $P \leq 0.05$, ** = $P \leq 0.01$, *** = $P \leq 0.001$, **** = $P \leq 0.0001$.

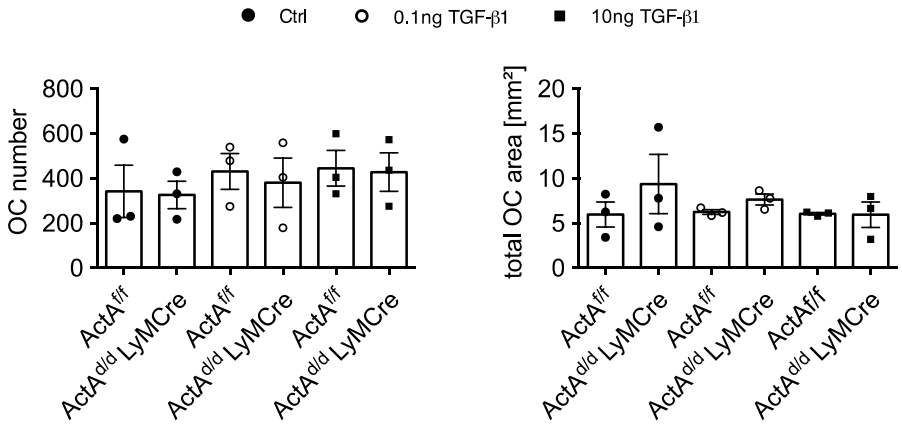

Supplementary figure S1: No influence of TGF-ß1 on RANKL-induced OC differentiation.

a) OC differentiation for 5 days in the presence of M-CSF (30 ng/mL) and RANKL (50 ng/mL) with or without (Ctrl) various concentrations of TGF-ß1. Quantification of OC numbers and total OC area (n = 3). **b)** OC differentiation for 5 days in the presence of CM from non-stimulated (Ctrl) and TGF-ß1 stimulated BMM. CM were obtained from experiments displayed in Figure 1i. Quantification of OC numbers and total OC area (n = 3). All data are means ± SEM (2-way ANOVA, Bonferroni's multiple comparison test).

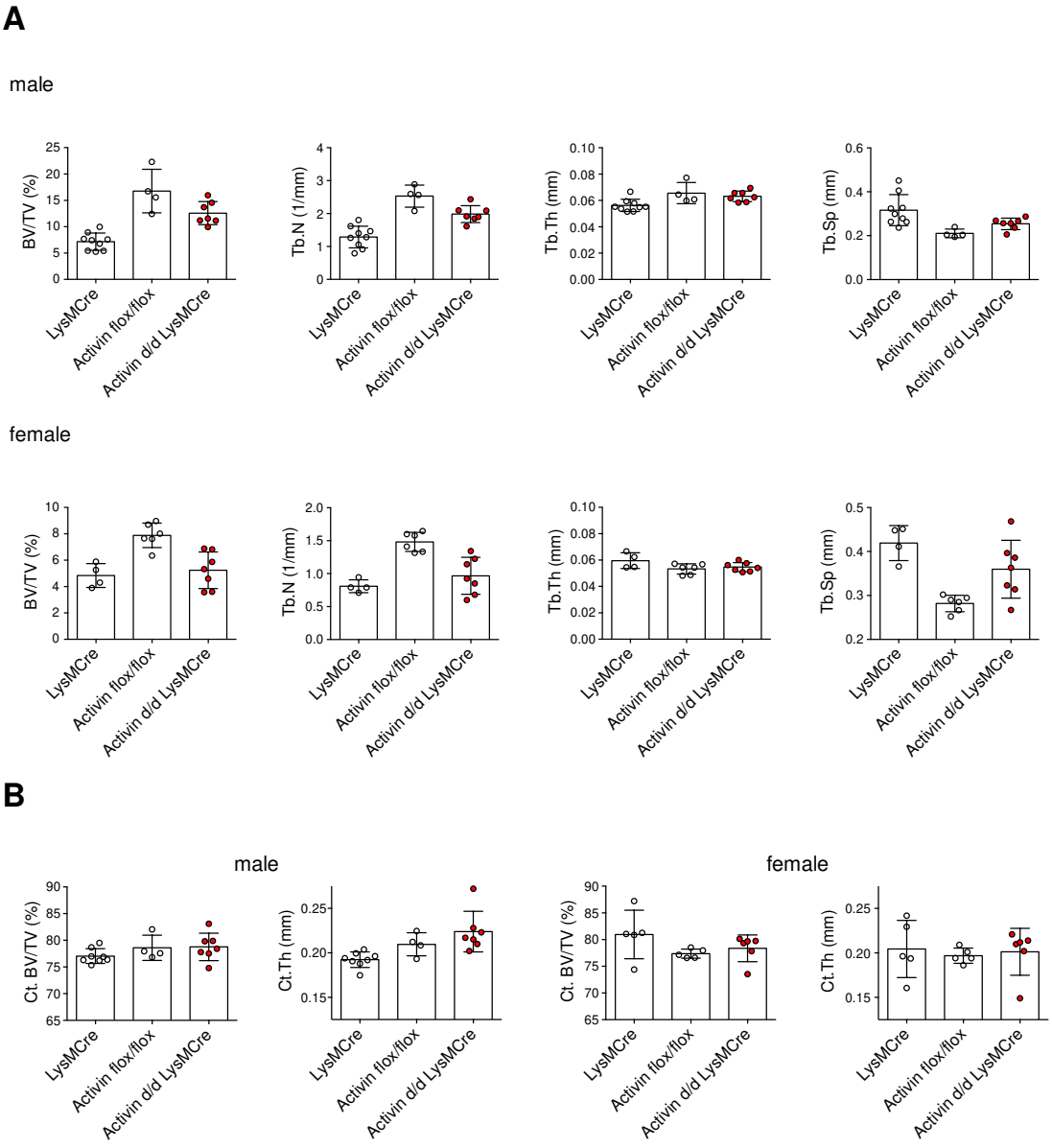

Supplementary figure S2: Physiological bone remodeling is not affected by deletion of activin A in myeloid cells.

Bone parameters were measured in 12 weeks old mice using micro-computed tomography. **A)** Trabecular bone parameters: bone volume fraction (BV/TV), trabecular number (Tb.N), trabecular thickness (Tb.Th), trabecular separation (Tb.Sp). **B)** cortical bone parameters: cortical bone volume fraction (Ct.BV/TV), cortical thickness (Ct.Th). All data are means ± SD (2-way ANOVA, Bonferroni's multiple comparison test).

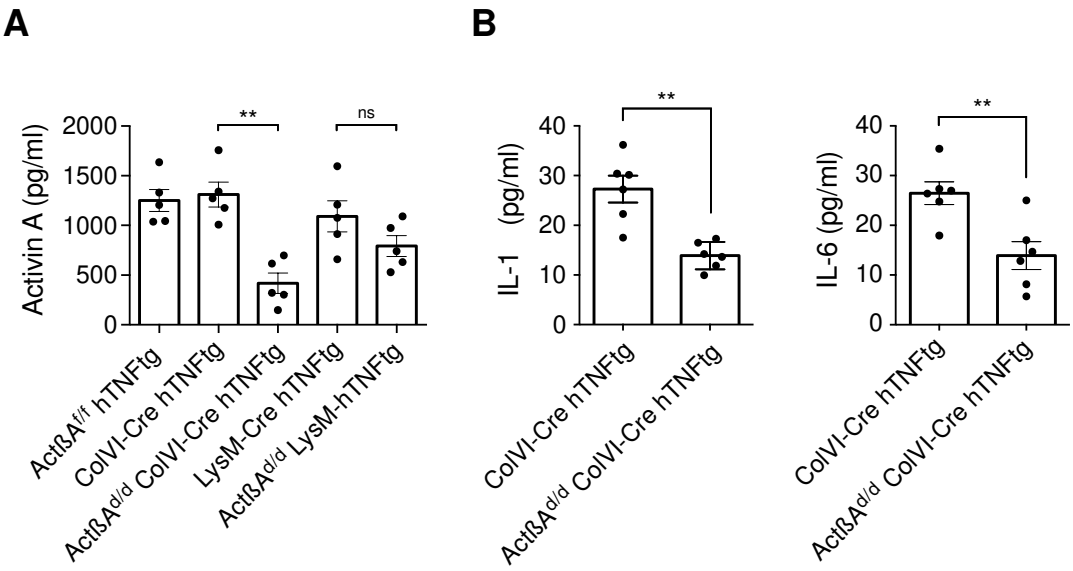

Supplementary figure S3: Serum levels of activin A, IL-1, and IL-6 are highly reduced in ActßA$^{d/d}$ ColVI-Cre hTNFtg mice.

A) Activin A concentrations in serum of arthritic mice with or without cell-specific deletion of activin A. Data represent means ± SEM (n = 5, ANOVA, Bonferroni's multiple comparison test unpaired t-test, ** = P ≤ 0.01). **B)** Serum concentrations of IL-1α and IL-6 in ColVI-Cre and ActßA$^{d/d}$ ColVI-Cre arthritic mice. Data represent means ± SEM (Mann-Whitney U test, ** = P ≤ 0.01).

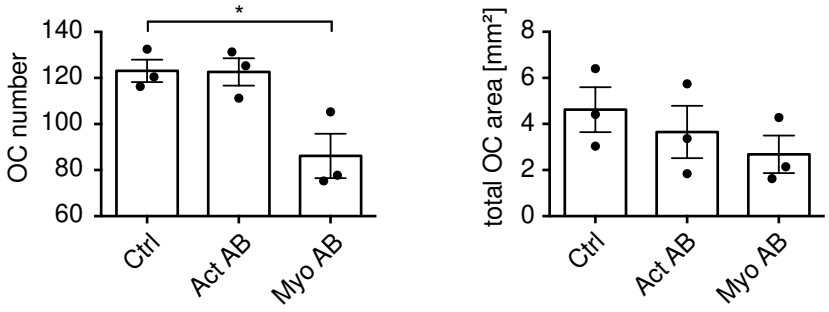

Supplementary figure S4: Blocking myostatin but not activin A reduce OC development in mono-cultures of ActβA$^{d/d}$ LysM-Cre BMDMs.

OC number and area after 6 days of OC differentiation in the presence of 30 ng/mL M-CSF and 50 ng/mL RANKL in the absence (Ctrl) or presence of anti-activin antibody or anti-myostatin antibody (n = 3). All data are means ± SEM (paired t-test, * = P ≤ 0.05).

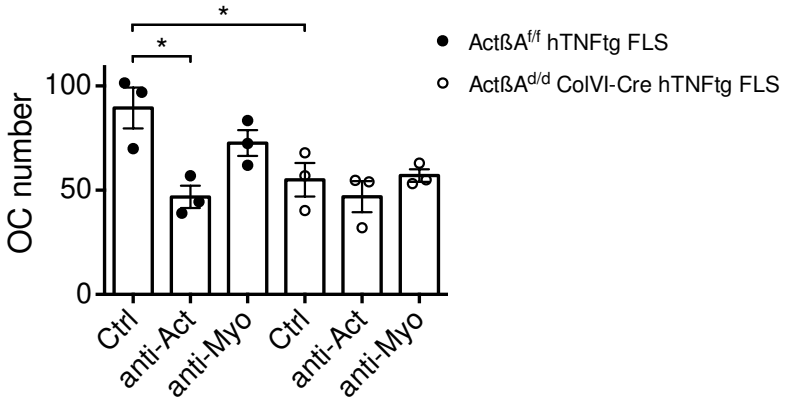

Supplementary figure S5: Blocking of activin A but not of myostatin led to reduced OC formation in co-cultures of BMDMs and arthritic FLS.

WT BMDMs co-cultured with FLS from ActβA$^{f/f}$ hTNFtg and ActβA$^{d/d}$ ColVI-Cre hTNFtg mice for 6 days in the absence (Ctrl) or presence of anti-activin or anti-myostatin antibody (n = 3). All data are means ± SEM (ANOVA (within one genotype), Mann-Whitney U test (between different genotypes), * = P ≤ 0.05).

ActßA$^{f/f}$ hTNFtg

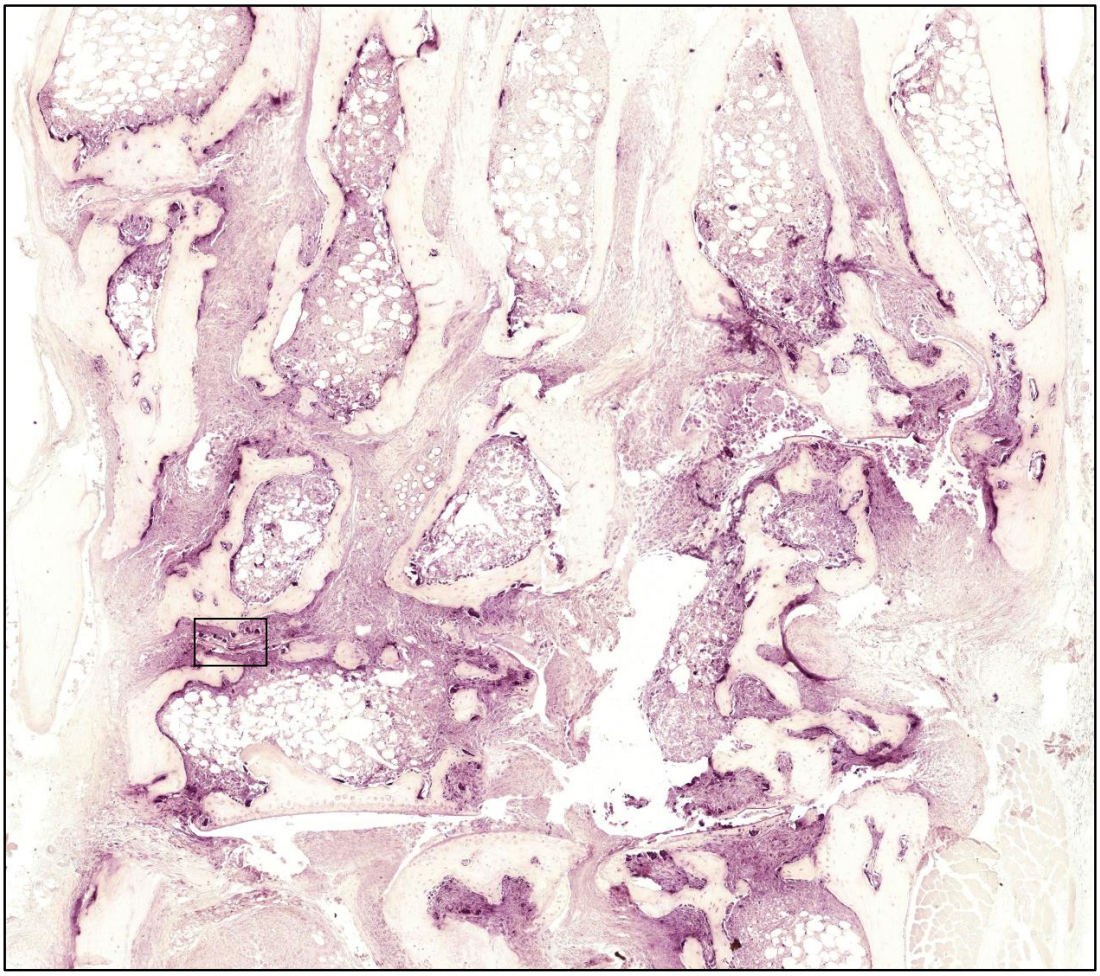

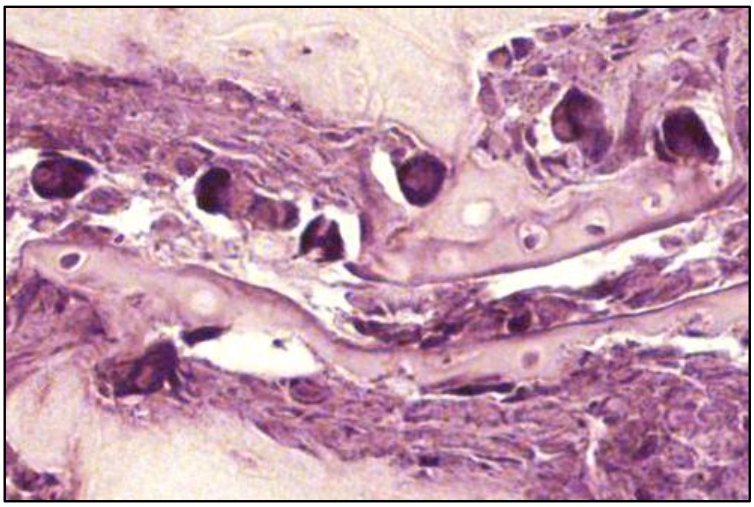

ActßA$^{d/d}$ LysM-Cre hTNFtg

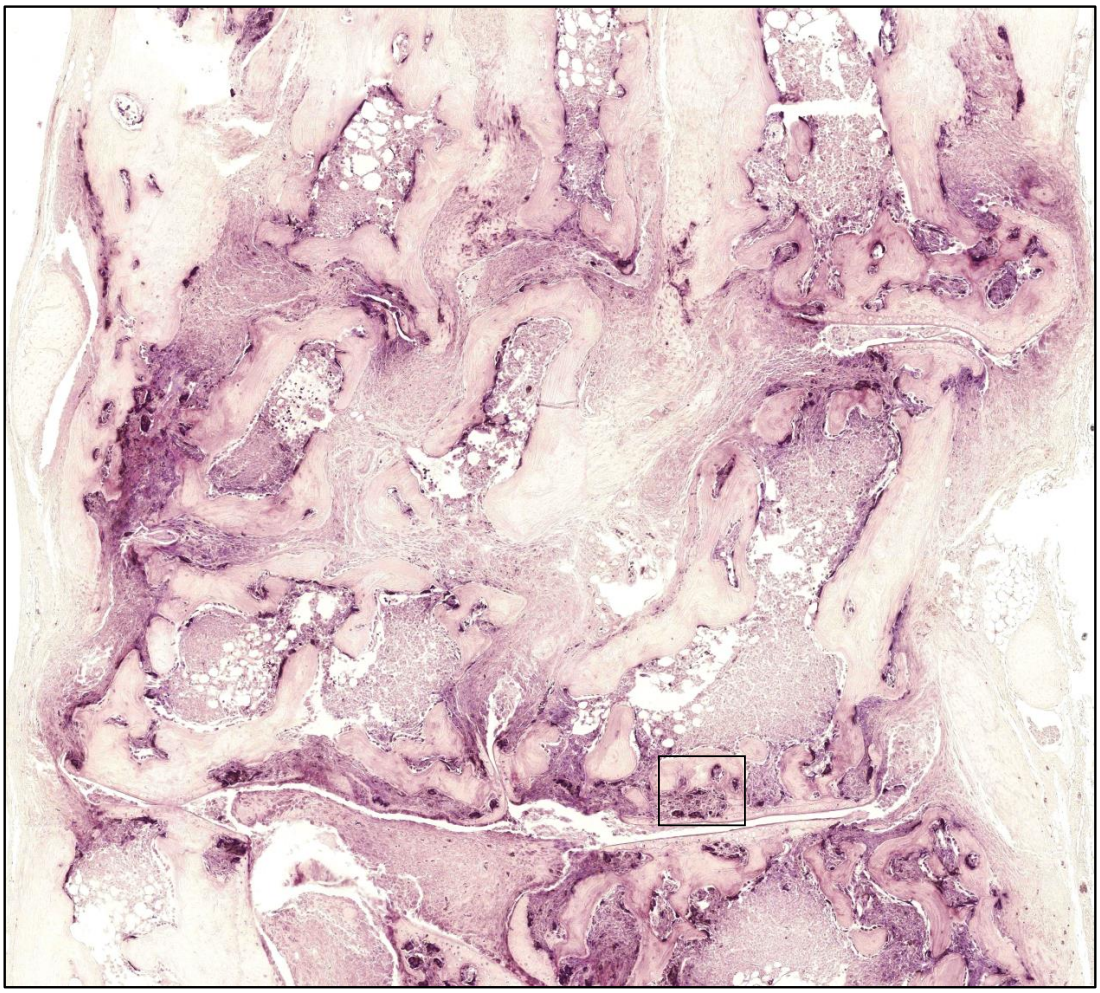

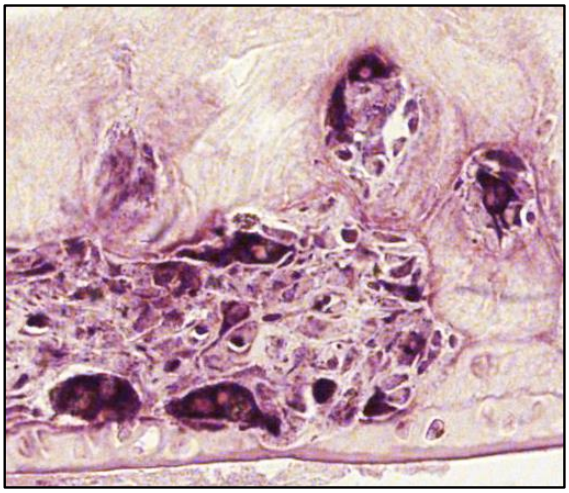

ActβA$^{d/d}$ ColVI-Cre hTNFtg

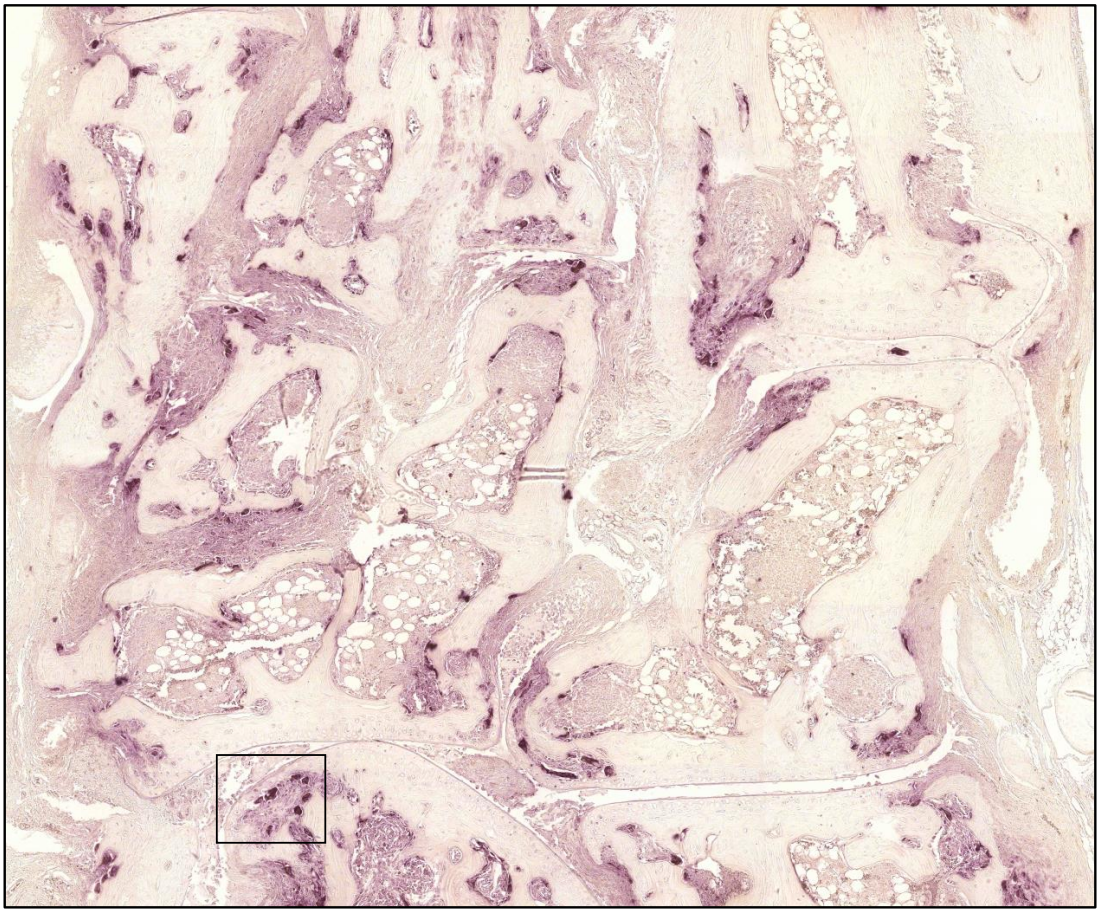

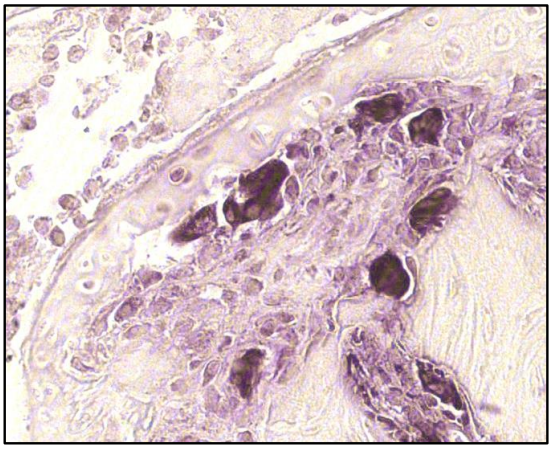

Supplementary figure S6: High resolution images of TRAP stainings from hindpaws of ActβA$^{f/f}$ hTNFtg, ActβA$^{d/d}$ LysM-Cre hTNFtg and ActβA$^{d/d}$ ColVI-Cre hTNFtg mice from Figures 4 and 6.

Deletion of activin A in mesenchymal but not myeloid cells ameliorates disease severity in experimental arthritis

Vanessa Waltereit-Kracke[1], Corinna Wehmeyer[1], Denise Beckmann[1], Eugenie Werbenko[1], Julia Reinhardt[1], Fabienne Geers[1], Mike Dienstbier[1], Michelle Fennen[1], Johanna Intemann[1], Peter Paruzel[1], Adelheid Korb-Pap[1], Thomas Pap[1], Berno Dankbar[1]

[1]WWU Muenster, Institute of Musculoskeletal Medicine (IMM), Muenster, Germany

Corresponding author (to whom also reprint requests should be sent):
Berno Dankbar, PhD
Institute of Musculoskeletal Medicine
University Hospital Muenster
Albert-Schweitzer-Campus 1, Bldg. D3
D-48149 Muenster
Germany
Phone: +49-251-835 6756
Fax: +49-251-835 7462
Email: dankbarb@uni-muenster.de

Supplemental material

Methods

Human synovial tissues and cells. All studies with human samples were approved by the ethics committee of University Hospital Münster. Synovial tissues from patients with RA or OA (according to the 1987 revised American College of Rheumatology criteria for RA and OA) were obtained during joint replacement surgery (Department of Orthopaedic Surgery, St. Joseph Hospital, Sendenhorst, Germany; Department of Orthopeadic Surgery of the University of Magdeburg School of Medicine, Magdeburg, Germany; Department of Orthopeadic Surgery, KMG-Kliniken Kyritz, Germany). All patients submitted informed consent prior to surgery. Human synovial fibroblasts were isolated by enzymatic digestion of synovial tissues using dispase II, cultured in DMEM with 10 % FCS and were used between passages 4 and 7. Human peripheral blood mononuclear cells (PBMC) were isolated from peripheral blood using Histopaque-1077 (Merck, Darmstadt, Germany) according to the manufacturer's instructions.

Animals. Actβ$A^{flox/flox}$, LysM-Cre (provided by University Hospital, Münster, Germany) and ColVI-Cre mice have been described previously[32–34]. Actβ$A^{flox/flox}$ mice were mated with Cre mice in order to obtain Actβ$A^{d/d}$ LysM-Cre and Actβ$A^{d/d}$ ColVI-Cre mice. These mice were then crossbred with hTNFtg mice (strain Tg197[35]) to obtain arthritic mice with cell-specific deletions of activin A. Mice were sacrificed at the age of 12 weeks. All mouse strains were kept at the C57BL/6J genetic background. Standard animal husbandry in accordance with the institutional guidelines was performed to generate cohorts of male and female mice. All animal procedures have been approved by the local ethics committee „Landesamt für Natur, Umwelt und Verbraucherschutz

Nordrhein-Westfalen“ (LANUV; 84.02.04.2017.A112) and were carried out in compliance with the ARRIVE guidelines.

Immunofluorescence staining. Human and murine tissue samples were fixed in 4 % paraformaldehyde overnight, embedded in paraffin and cut into 5 µm sections. Murine hind paws were additionally decalcified in ammonium EDTA before embedding in paraffin. Deparaffinized sections were rehydrated and antigen retrieval was performed with 1x Trypsin/EDTA (PAA Laboratories, Pasching, Austria) in a humid chamber for 10 minutes at 37°C or incubated with citrate buffer (pH 2,5) in a humid chamber for 2 hours at RT. After digestion, the samples were washed with TBS. Afterwards the tissues were blocked in 10% horse serum for an hour. Sections were stained with primary antibodies, goat polyclonal to Activin A (R&D #AF338, dilution 1:50), mouse monoclonal to CD68 (Abcam #ab955, dilution 1:100), rabbit monoclonal to Myeloperoxidase (Abcam #ab208670, dilution 1:200) or rabbit polyclonal to Thy1/CD90 (LSBio #LS-C414760, dilution 1:100) overnight by 4°C. After washing with TBS, slices were incubated with secondary antibodies anti-goat 488 (Invitrogen #A-11055, dilution 1:5000), anti-mouse 555 (Invitrogen #A-31570, dilution 1:5000) and anti-rabbit 647 (Invitrogen #A-21245, dilution 1:5000) for an hour, counterstained with DAPI (Invitrogen #D1306, dilution 1:10.000) and mounted in aqueous mounting media.

Murine fibroblasts and bone marrow cells. Murine FLS were isolated from deskinned hind paws of 12-week old mice by enzymatic digestion with collagenase type IV (Worthington-Biochemical Corporation, Lakewood, USA) and cultured in DMEM with 10 % FCS at 37 °C and 5 % CO_2. To avoid contamination with other cells, passages 3 to 5 were used for further experiments. Murine bone marrow cells (BMCs) were isolated from femora and tibiae from 6- to 12-week old mice by flushing out BM

cells of the marrow cavity and cultivating them in α-MEM with 10 % FCS and 30 ng/mL M-CSF (R&D Systems, Nordenstadt, Germany) at 37 °C and 5 % CO_2 in order to differentiate them to BMDMs.

ELISA measurements. Concentrations of activin A, interleukin-1 alpha (mIL-1α) and interleukin-6 (mIL-6) in mouse serum and/or supernatants of stimulated and unstimulated FLS and BMDMs were analysed by Quantikine ELISA Kits (R&D Systems, Minneapolis, USA). All assays were performed according to the manufacturer's instructions.

Semi-quantitative PCR. Total RNA from human RA and hTNFtg FLS was isolated using peqGOLD TriFast™ (VWR, Radnor, USA) according to the manufacturer's instructions. Synthesis of cDNA was performed by using the iSkript™ cDNA Synthesis Kit (Bio-Rad Laboratories, Inc., Hercules, USA). The synthesized cDNA was used for PCR using human inhibin βA primers (forward CAT CAC GTT TGC CGA GTC AG, reverse GAC TGC TCC TTT TCC TCA TC) and GAPDH primers (forward TCC TGC ACC ACC AAC TGC TT, reverse TCC ACC ACC CTG TTG CTG TA) or the murine inhibin βA (forward GGG ACC CGA AAG AGA ATT TGC, reverse TCC TCT CAG CCA AAG CAA GG) and GAPDH primers (forward ATG TGT CCG TCG TGG ATC TG, reverse ATG TGT CCG TCG TGG ATC TG).

***In vitro* osteoclast generation and resorption assay.** Murine BMCs and human PBMCs were primed for 72 h with 30 ng/mL M-CSF (R&D Systems, Minneapolis, USA) followed by stimulation with 30 ng/mL M-CSF and 50 ng/mL RANKL (R&D Systems, Minneapolis, USA) for further 4 to 6 days (murine) or 15 days (human). To analyse the impact of activin A on OC formation 30 ng/mL or 100 ng/mL activin A (R&D Systems,

Minneapolis, USA) was added to WT BMDMs or PBMCs, respectively. Additionally, the impact of TGF-ß1 on OC formation was evaluated by incubation of WT BMDMs with 0.1 and 10 ng/mL TGF-ß1 (R&D Systems, Minneapolis, USA). To inhibit activin A-mediated receptor signaling, a specific ALK4/5/7 inhibitor (SB431542, Sigma-Aldrich, St. Louis, USA) with a concentration of 5 µM was used. To assess the toxicity of the inhibitor, recovery experiments were performed in which the inhibitor was removed, cells were washed with PBS and stimulated with 30 ng/mL M-CSF and 50 ng/mL RANKL with or without 30 ng/mL activin A. For inhibition experiments, cells were incubated with anti-activin A (0.3 µg/mL, R&D Systems) or anti-GDF-8 (3 µg/mL, R&D Systems) antibodies. OC formation was determined by TRAP staining (Acid Phosphatase, Leukocyte (TRAP) Kit, Sigma-Aldrich, St. Louis, USA).

Bone resorption assays were performed by seeding the cells on a calcium phosphate-coated 48-well plate followed by priming and stimulation as described for the OC differentiation. Afterwards, cells were removed by treating the wells with 5 % sodium hypochlorite and washed three times with PBS. For quantification of resorption pits, the entire wells were recorded with the Axio Observer Z1. The area of resorption pits was measured using ZEN 2 software.

Assessment of proliferation. For assessment of proliferation of BMDMs, cells were cultured with M-CSF (30 ng/mL) and with or without activin A (30 ng/mL) for 1, 2 and 3 days. Afterwards, cells were fixed with 4 % PFA for 15 min at RT, washed with PBS and stained for DAPI. The number of cells was determined by counting the DAPI stained cells in ImageJ.

Micro-CT and histomorphometric analysis. Hind paws of mice were fixed in 4 % PFA at 4 °C for 24 h and washed with PBS followed by scanning with Skyscan 1176

high resolution *in vivo* microtomograph (Bruker, Billerica, USA). The data were reconstructed by using NRecon v1.6.10.4 (Bruker, Billerica, USA) and exported as three-dimensional data by using CT Analyser v.1.16.4.1 (Bruker, Billerica, USA). The samples were shaded in MeshLab v2016.12 (Visual Computing Laboratory, Pisa, Italy) using ambient occlusion and snapshots were taken. For evaluation of trabecular and cortical bone parameters, images were reconstructed using the software NRecon v1.7.3.2 and analysed using the CTan v1.17.7.2.

Histomorphometric analysis was performed on toluidine-blue and TRAP stained paraffin sections. Images were taken of the tarsal joints of the hind paws using the Axio Observer Z1 microscope. Quantification was conducted with the ZEN software as described before [36]. Briefly, the area of inflammation was calculated on toluidine blue-stained sections as the sum of areas of inflamed tissue in tarsal joints in relation to the total tarsal joint area. To determine bone erosion, the area of bone loss was quantified on the same toluidine-blue stained section in relation to the total tarsal joint area. OCs were counted in TRAP-stained sections.

Co-Cultures. For co-cultures $5x10^3$ FLS were seeded in a 96-well containing FLS culture medium. On the next day, $1x10^5$ EGFP-BMCs were seeded onto the FLS layer and cultured for 3 - 6 days in OC medium containing 1 µM prostaglandin E_2 (PGE_2). OC differentiation was stopped by fixing the cells with 4 % PFA. For inhibition experiments, anti-activin A (0.3 µg/mL) and anti-myostatin (3 µg/mL) antibodies were applied (both R&D Systems). OC number was determined by visualizing the fixed cells by fluorescence using the Axio Observer Z1 and ZEN 2 software.

Co-immunoprecipitation. Co-Immunoprecipitation experiments were performed via Dynabeads™ Protein G according to the manufacturer's protocol. Phospho-Smad2

antibody was coupled to protein G-labelled Dynabeads. Equal amounts of cell lysates were transferred to the bead-bound antibody and incubated for 90 min at RT. Subsequent Western blot analysis against NFATc1 was performed.

Immunoblotting. Total protein lysates or co-immunoprecipitates were electrophoretically separated by 80 V for 1 - 2 h. Subsequent protein transfer to Trans-Blot® Turbo™ Mini PVDF membranes was carried out electrophoretically at 25 V for 3 min. PVDF membranes were blocked with BSA-based blocking solution for 1h at RT. The primary antibody was incubated overnight at 4 °C under continuous rotation. Afterwards, membranes were washed three times with TBS-T for 5 min followed by incubation with HRP-linked secondary antibody for 1h at RT under continuous rotation. Membranes were washed, incubated with ECL solution for 2 min, and protein of interest was visualized via chemiluminescence signaling using a Fusion FX Western blot imager.

Statistical analysis. All data are presented as means ± SEM or ± SD. Statistical analysis was performed using GraphPad Prism 7 software. Paired data were analysed by paired t-test, unpaired data were analysed by unpaired t-test or a Mann-Whitney-U test. If a t-test was used, the data were tested for normality using a D'Agostino & Person normality test or, in the case that the n-number was too small, a Shapiro-Wilk normality test was applied. In case of three or more groups, data were statistically analysed by ANOVA followed by Bonferroni's multiple comparison test. P-values ≤ 0.05 were considered as significant. * = $P \leq 0.05$, ** = $P \leq 0.01$, *** = $P \leq 0.001$, **** = $P \leq 0.0001$.

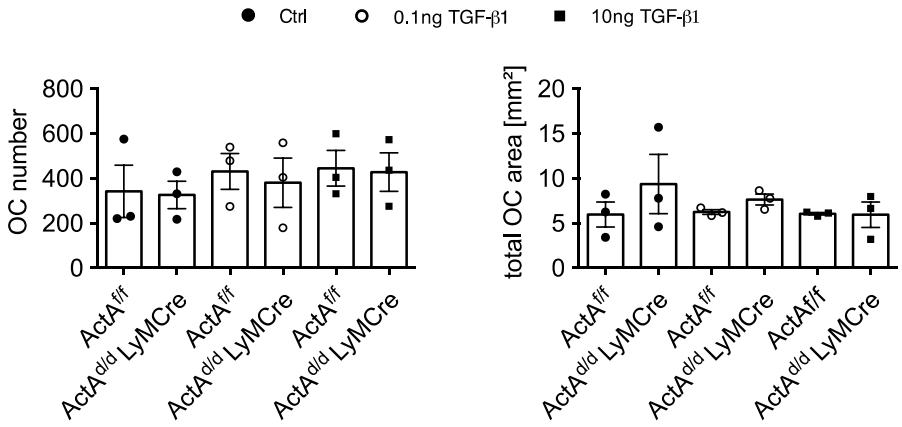

Supplementary figure S1: No influence of TGF-ß1 on RANKL-induced OC differentiation.

a) OC differentiation for 5 days in the presence of M-CSF (30 ng/mL) and RANKL (50 ng/mL) with or without (Ctrl) various concentrations of TGF-ß1. Quantification of OC numbers and total OC area (n = 3). **b)** OC differentiation for 5 days in the presence of CM from non-stimulated (Ctrl) and TGF-ß1 stimulated BMM. CM were obtained from experiments displayed in Figure 1i. Quantification of OC numbers and total OC area (n = 3). All data are means ± SEM (2-way ANOVA, Bonferroni's multiple comparison test).

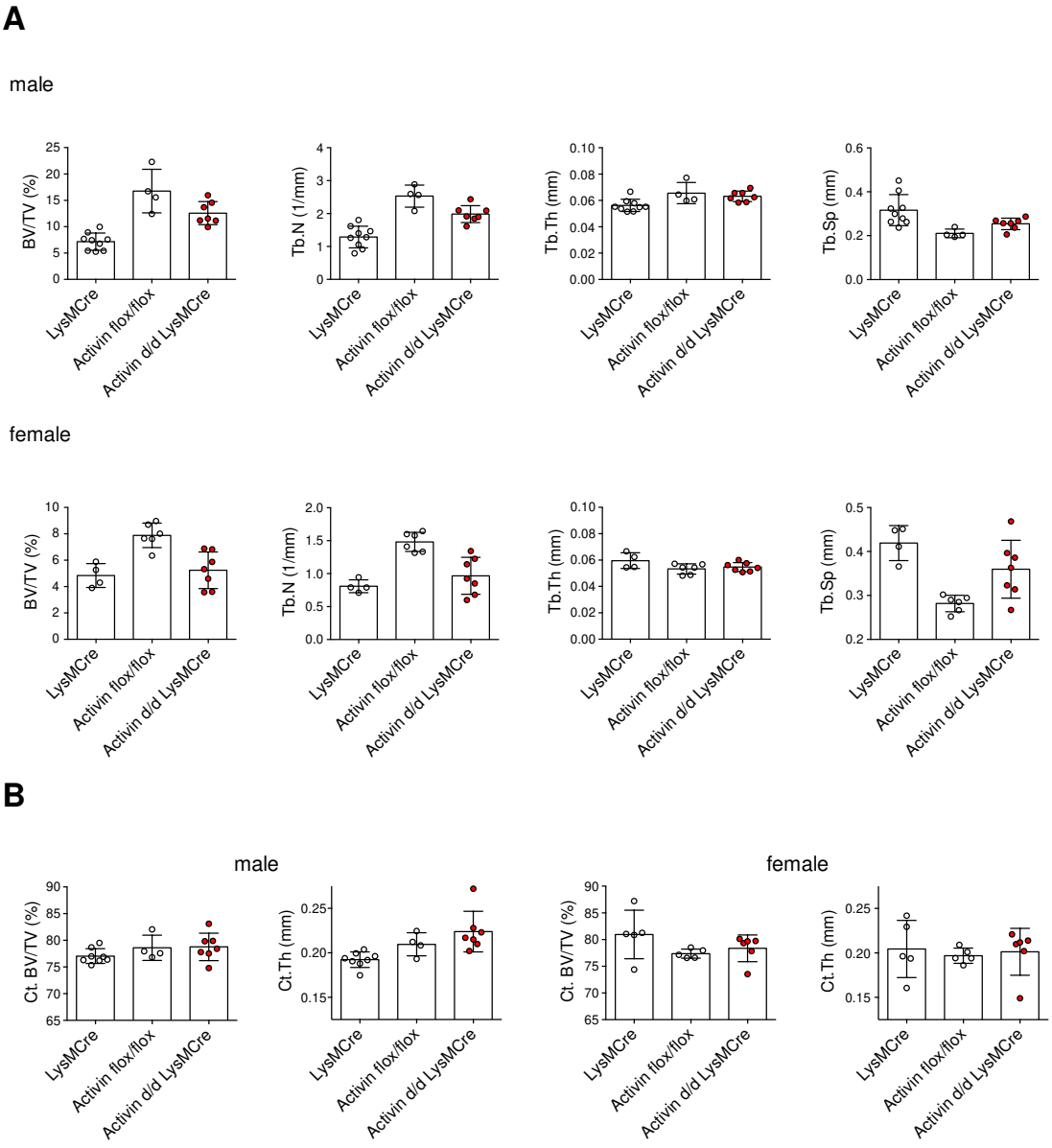

Supplementary figure S2: Physiological bone remodeling is not affected by deletion of activin A in myeloid cells.

Bone parameters were measured in 12 weeks old mice using micro-computed tomography. **A)** Trabecular bone parameters: bone volume fraction (BV/TV), trabecular number (Tb.N), trabecular thickness (Tb.Th), trabecular separation (Tb.Sp). **B)** cortical bone parameters: cortical bone volume fraction (Ct.BV/TV), cortical thickness (Ct.Th). All data are means ± SD (2-way ANOVA, Bonferroni's multiple comparison test).

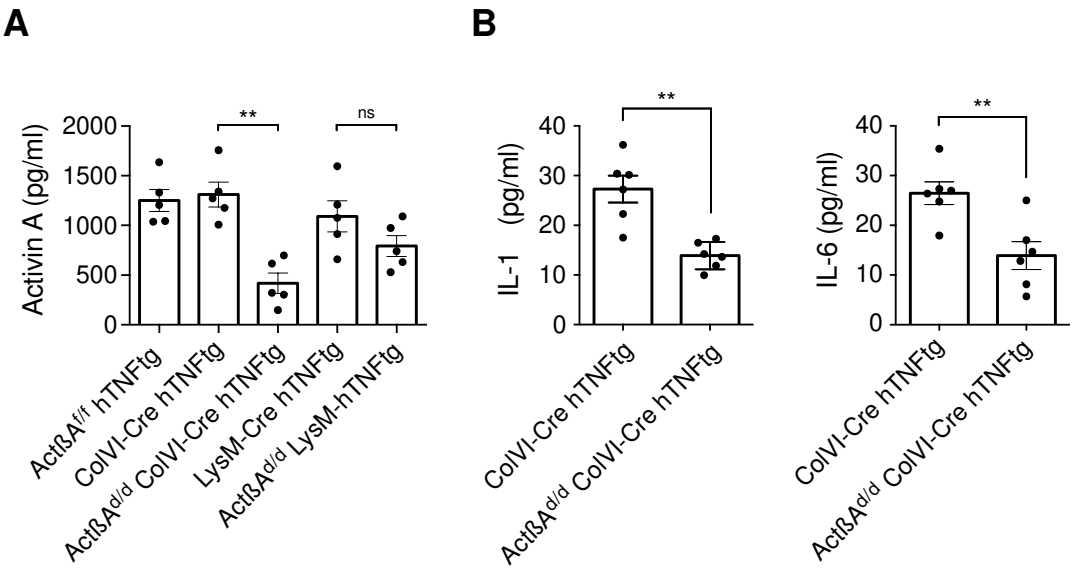

Supplementary figure S3: Serum levels of activin A, IL-1, and IL-6 are highly reduced in ActßA$^{d/d}$ ColVI-Cre hTNFtg mice.

A) Activin A concentrations in serum of arthritic mice with or without cell-specific deletion of activin A. Data represent means ± SEM (n = 5, ANOVA, Bonferroni's multiple comparison test unpaired t-test, ** = P ≤ 0.01). **B)** Serum concentrations of IL-1α and IL-6 in ColVI-Cre and ActßA$^{d/d}$ ColVI-Cre arthritic mice. Data represent means ± SEM (Mann-Whitney U test, ** = P ≤ 0.01).

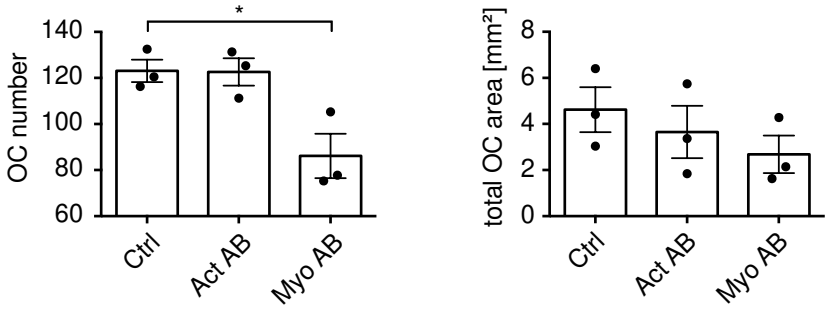

Supplementary figure S4: Blocking myostatin but not activin A reduce OC development in mono-cultures of ActβA$^{d/d}$ LysM-Cre BMDMs.

OC number and area after 6 days of OC differentiation in the presence of 30 ng/mL M-CSF and 50 ng/mL RANKL in the absence (Ctrl) or presence of anti-activin antibody or anti-myostatin antibody (n = 3). All data are means ± SEM (paired t-test, * = P ≤ 0.05).

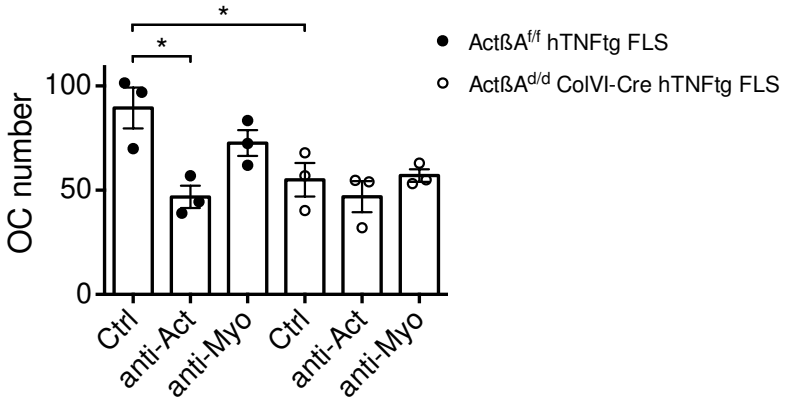

Supplementary figure S5: Blocking of activin A but not of myostatin led to reduced OC formation in co-cultures of BMDMs and arthritic FLS.

WT BMDMs co-cultured with FLS from ActβA$^{f/f}$ hTNFtg and ActβA$^{d/d}$ ColVI-Cre hTNFtg mice for 6 days in the absence (Ctrl) or presence of anti-activin or anti-myostatin antibody (n = 3). All data are means ± SEM (ANOVA (within one genotype), Mann-Whitney U test (between different genotypes), * = P ≤ 0.05).

ActßA$^{f/f}$ hTNFtg

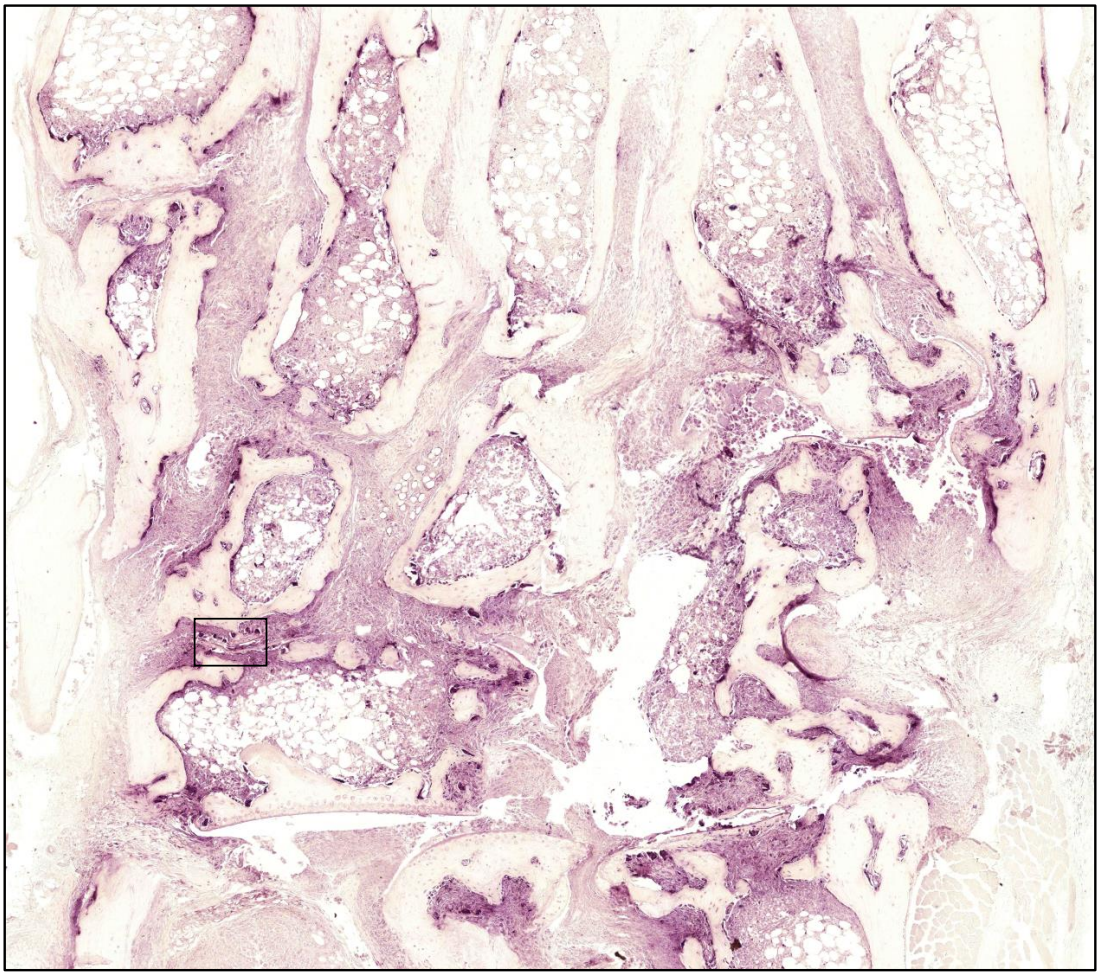

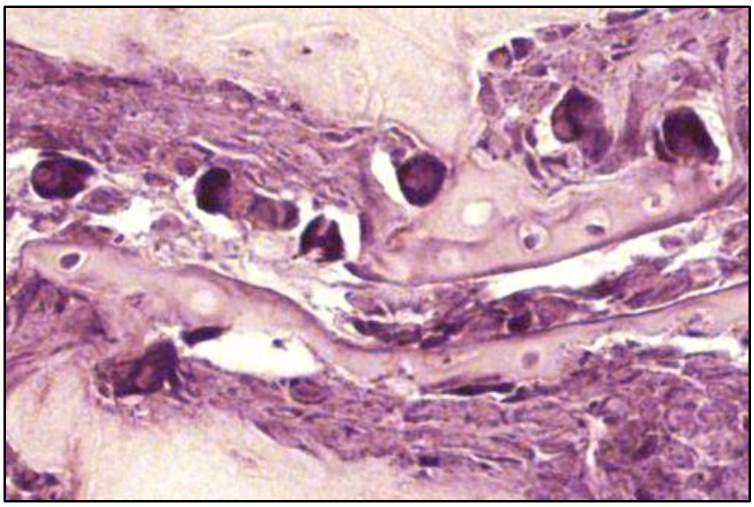

ActßA$^{d/d}$ LysM-Cre hTNFtg

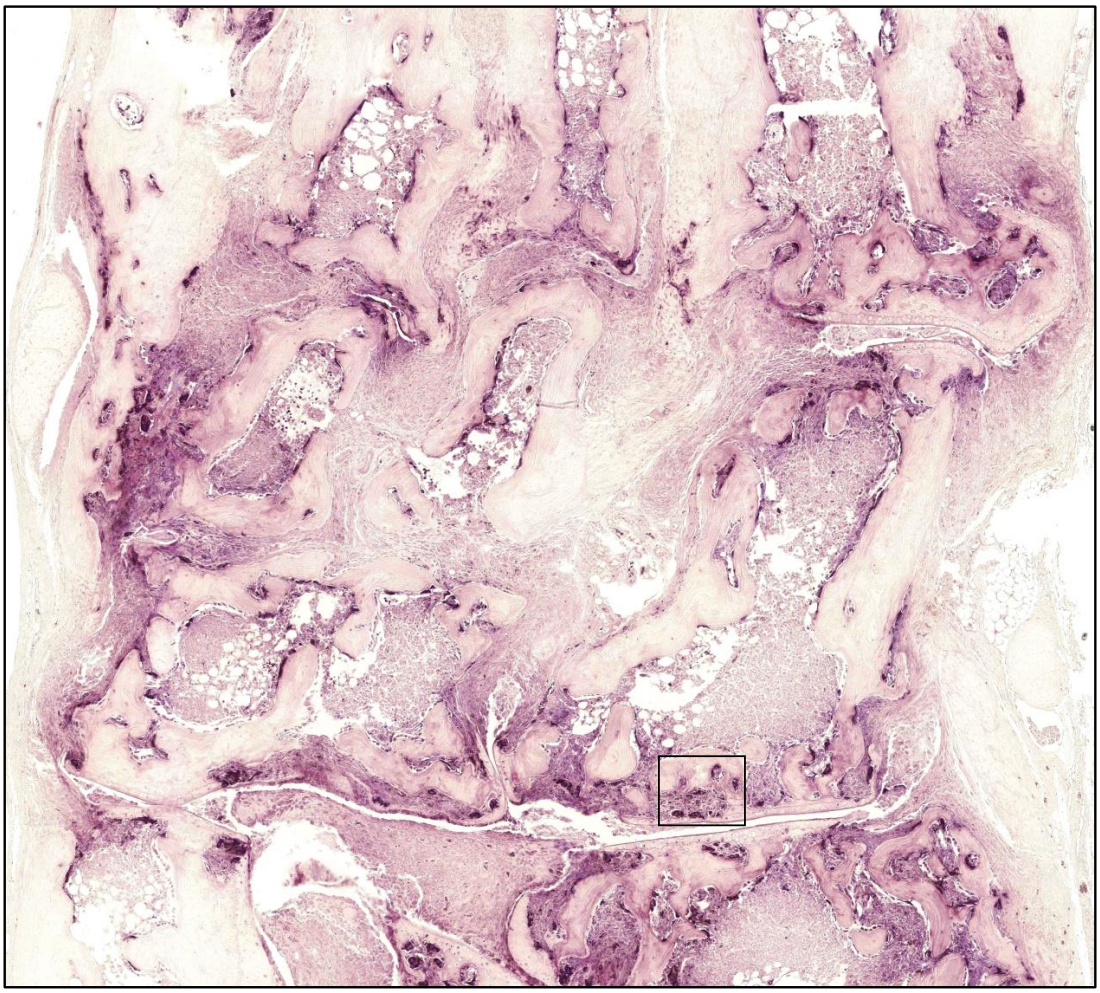

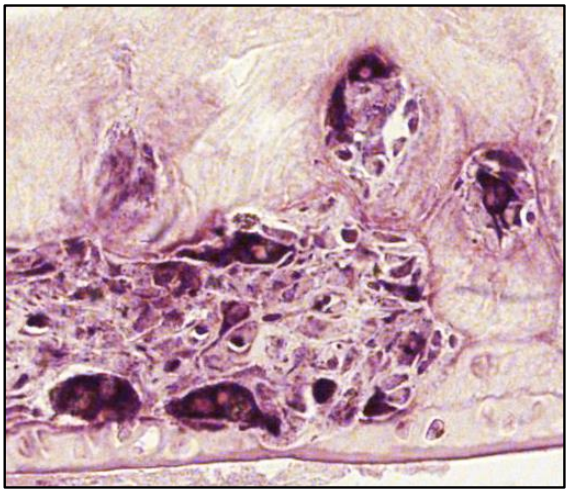

ActβA$^{d/d}$ ColVI-Cre hTNFtg

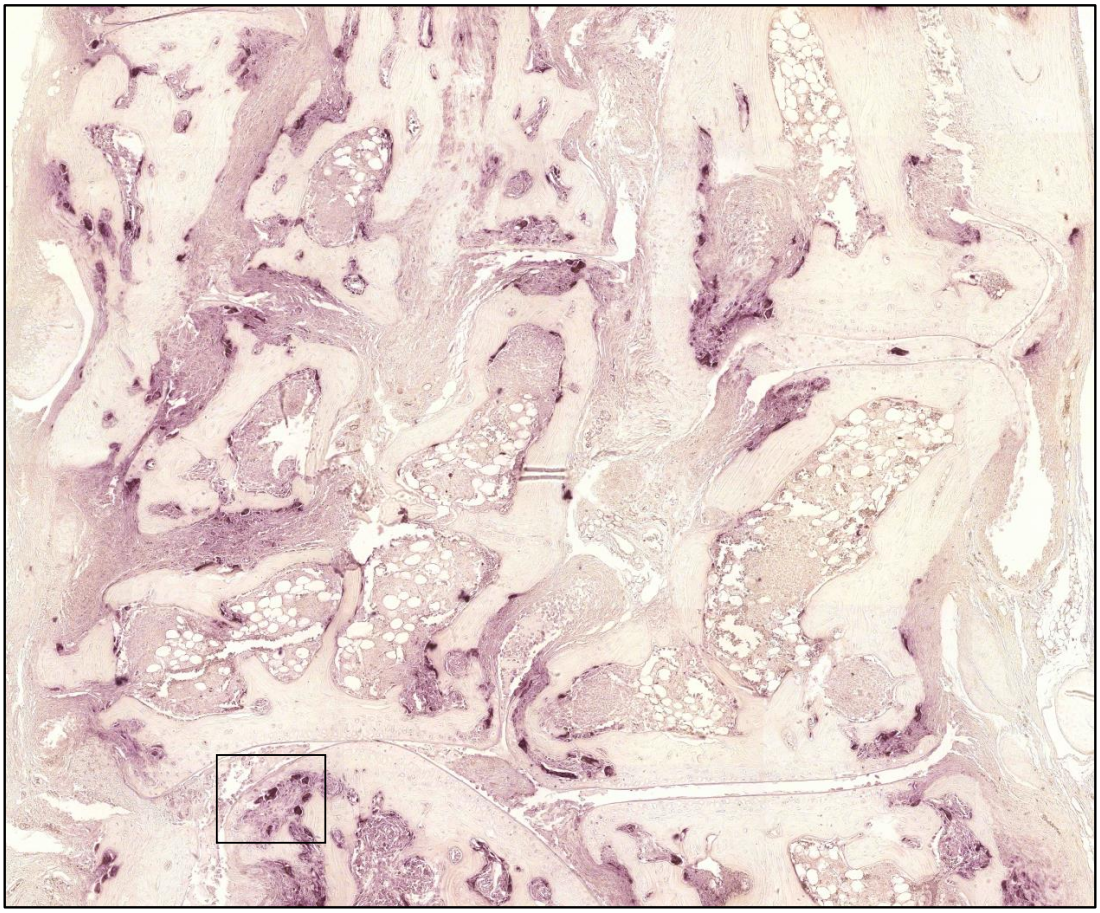

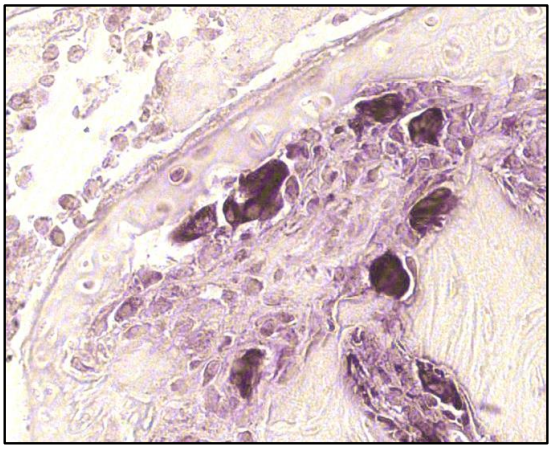

Supplementary figure S6: High resolution images of TRAP stainings from hindpaws of ActβA$^{f/f}$ hTNFtg, ActβA$^{d/d}$ LysM-Cre hTNFtg and ActβA$^{d/d}$ ColVI-Cre hTNFtg mice from Figures 4 and 6.